

Anonymous Referee #1

This manuscript analyses the variability in CHBr₃, as one of the major VSLs Bromine species that can be transported to the stratosphere by strong convection in the tropical latitudes. They have used a representative surface emission pattern at monthly-mean time intervals, and transport-chemistry parameterized using FLEXPART, a widely used modelling system for short-lived species simulation. The manuscript is generally very well written, and the subject of this research is important. However, I have some strong reservations which have to be addressed before manuscript can be accepted for publication in ACP.

We thank Referee 1 for his/her valuable comments. We have changed the manuscript according to the comments listed below and think that these changes have improved the quality of the manuscript.

Major comments.

I am very concerned with the model simulation over the South Asia region. The pattern of transport of VSLs species from the surface layers appears unrealistic (Fig. 8), meaning the location of the anticyclone in JJA appears to be vastly misplaced for both CHBr₃ and Transit time, based on our knowledge of global (Eulerian) chemistry-transport models and observation of tracers, e.g., Park et al. (JGR, 2007) or Chandra et al. (ACP, 2017). The upward motion over the India monsoon domain is limited to northern India rather than in the tropical areas.

The referee is correct that during boreal summer, the centre of the anticyclone is situated over the continental part of Asia extending from the Tibetan Plateau to the Middle East and north-eastern Africa. As various modelling and observational studies have demonstrated, intense convection can loft boundary layer pollutants and aerosols into the upper troposphere/lower stratosphere anticyclone. Here the polluted air masses remain mostly confined within the closed circulation of the anticyclone for days to weeks

When comparing this current state of knowledge with our results, it is important to keep in mind that 1) nearly all studies focus on pollutants emitted over the Asian land masses and not on oceanic trace gases and vice versa 2) air masses found in the anticyclone mostly originate from the planetary boundary and not from the marine boundary layer.

The second point is demonstrated by Bergmann et al. (2013) who state: ‘ ... We calculated regional contributions to air within the anticyclone by boundary layer sources from five regions: the Tibetan Plateau, India/SE Asia, eastern China, the Indian Ocean, and the western Pacific. ... Boundary layer sources for the anticyclone are primarily from the Tibetan Plateau and India/SE Asia (a combined 70%–80%) at both the 200 mbar and 100 mbar levels, with minor contributions by the western Pacific and Indian Ocean (a combined 15%–20%). ... ’

Furthermore Vogel et al. (2018) based on CLAMS backward simulations of the anticyclone states '... High fractions of air from India/China up to 90 % and low fractions below 10 % from the tropical adjacent regions are found in the core of the Asian monsoon anticyclone at 360 K potential temperature. Highest fractions from the tropical adjacent regions of about 40 % are found in a belt around the edge of the anticyclone ...'

In consequence the stratospheric entrainment of an oceanic trace gas, like bromoform, over the South Asian region does not necessarily need to reflect the entrainment of anthropogenic pollutants like CO. As the air trapped in the anticyclone only contains a small fraction of marine boundary layer air, marine trace gases as short-lived as bromoform might not show a maximum in the anticyclone. Localized convection extending from the Arabian Sea to the Philippines including the Bay of Bengal and the Arabian Sea acting on a trace gas with large sources over the equatorial and inner tropical oceans can be expected to cause high entrainment over southern India and adjacent ocean. This is consistent with results presented in Fiehn et al. (2018), who used the same FLEXPART ERA-Interim model experiment set up as our study and found the main injection of bromoform during boreal summer over the southern tip of India associated with the high local oceanic sources and strong convection of the summer monsoon.

Which raises a wider question about the validity of the FLEXPART model framework implemented in the work. Can there be some independent tracer simulation to validate the model transport, say using Radon-222 or SF6 or CO for which we have better knowledge of model transport (Forster et al., 2007 could be using older version of the model, is your version same that work?). I am aware that the FLEXPART works reasonably well for the horizontal transport at regional scale but not sure whether suitable for such global model simulation.

FLEXPART has been successfully used in studies of transport and tracer distributions in the Asian monsoon (e.g., Lal et al., 2014; Lelieveld et al., 2018; Li et al., 2016). Some of these studies include comparisons to or evaluations of observational data. In previous related work, we have validated our VSLS FLEXPART ERA-Interim model set-up for the tropical West Pacific ship-aircraft-land campaign in November 2011 which showed very good agreement between modelled and observed VSLS profiles in this convection dominated area (Fuhlbruegge et al 2016 ACP; "The EU Project SHIVA" special issue ACP).

Validation of the convective scheme used in FLEXPART by Forster et al., 2007 is indeed based on an older version of FLEXPART compared to the one used in our paper. However, the convective scheme has not been changed in between versions, therefore the presented validation still applies to the current version of the model.

I am also very disappointed in the ways the model and measurements are compared. For a reasonable evaluation of the model simulations we need to first sample the model at the time and location of measurements.

We have improved our model-measurement comparisons by sampling the model output at the measurement time and location for comparisons in Figures 4 and 7. The new

comparison shows slightly different results; however, the overall findings do not change substantially.

Minor comments.

p.3, l#4: could you put a timeline here, as in the WMO/SAOD, 2018

Timeline and reference have been added.

p.3, l#13: may be cite - Hossaini et al., ACP, 2016

Reference has been added.

p.9, l#1ff: this is quite a bit of simplification of the loss of SGs, a proper treatment using a 3D OH field would have been useful to simulate tropospheric distribution of the SGs.

In general, FLEXPART simulations can also be carried out with the chemical loss term derived from the reaction with OH based on a prescribed 3D OH field. The chemical loss of bromoform, however, is largely driven by photolysis (Hossaini et al., 2010, Figure 4), which is not included in the current FLEXPART version. Therefore, the chemical loss is based on a lifetime profile derived from detailed chemistry simulations.

p. 11: Figure 1 and associated text: the southern spread of this anticyclone as appears from your figure looks too wide, is there a possibility to show these plots for summer and winter (arrange a 2x2 panel figure). The panel b doesn't provide sufficient information. Also, I would like you to add the surface fluxes for the two seasons, making it 2colx3row figure. Even though the emissions are taken from Ziska et al., the readers cannot directly assess results without showing here again.

We have added seasonal composites of the CHBr_3 concentrations at 17 km and of the air-sea fluxes from Ziska et al. (2013) to the supplementary material.

Figure 3 and associated text: Observations are much less than the model values

This is true for the AVE campaign but not for Pre-AVE or for ACCENT (see also the summarized comparison in Figure 4).

How to explain the spotty features in the model simulations?

The spotty features in the model simulations are a result of the high oceanic sources directly underneath interacting with localized convective transport. The latter brings localized air masses with very high bromoform mixing ratios from the boundary layer into the 15-17km layer. We have added this explanation to the manuscript.

Observations are higher over the Gulf of Mexico persistently, hinting towards low emissions?

Not necessarily, as the observations are in very good agreement for the Pre-AVE campaign and even lower for the AVE campaign

Figure 4 and associated text: I am not very happy with this comparison. I believe that the model simulations should be first sampled at the measurement points and then compared with measured values.

We have improved the comparison by adding model values sampled at the time and location of the measurements. We decided to also keep the averaged model values in the Figure in order to highlight the seasonal cycle and high tempo-spatial variability of CHBr₃ in the upper TTL suggested by the model results.

This plot makes me interpret that the model simulation is out of phase with the measurements during June to Aug! I do not know if this problem comes from not sampling the model properly or the model itself is wrong.

It is true that during the NH summer months 3 out of 4 campaigns show lower values. However, the ACCENT campaign shows much higher values. Most important, the standard deviation of the model results suggest higher variability during this time which is confirmed by the relatively large differences between the individual campaigns. Given the latter it is not clear if the model overestimates the NH summer entrainment. The manuscript states “... For the campaigns during NH summer, mean differences are larger in most cases. At the same time, the temporal and spatial variability of the simulated CHBr₃ distribution is also larger so that nearly all observations fall within the simulated uncertainty. The large differences between the individual campaigns during NH summer confirm the increased variability suggested by the model results. ...”.

p.21, l18: Again, good to have shown the emission maps in Fig. 1, for winter and summer.

We have added seasonal composites of the air-sea fluxes from Ziska et al. (2013) to the supplementary material and added a reference to the text.

Figure 7 and associated text: This again reiterate why are you not showing one-to-one comparison, given that the transport varies

We have improved the comparison by adding model values sampled at the time and location of the measurements. The new comparison shows slightly different results; however, the overall findings do not change substantially.

References:

- Bergman, J. W., Fierli, F., Jensen, E. J., Honomichl, S., and Pan, L. L. (2013), *Boundary layer sources for the Asian anticyclone: Regional contributions to a vertical conduit*, *J. Geophys. Res. Atmos.*, 118, 2560–2575, doi:10.1002/jgrd.50142.
- Engel, A., Rigby, M. (Lead Authors), Burkholder, J. B., Fernandez, R. P., Froidevaux, L., Hall, B. D., Hossaini, R., Saito, T., Vollmer, M. K. and Yao, B.: *Update on Ozone-Depleting Substances (ODSs) and Other Gases of Interest to the Montreal Protocol, Chapter 1*, in *Scientific Assessment of Ozone Depletion: 2018, Global Ozone Research and Monitoring Project – Report No. 58.*, 2018.
- Fiehn, A., Quack, B., Marandino, C. A., and Krüger, K., *Transport variability of very short lived substances from the West Indian Ocean to the stratosphere*. *Journal of Geophysical Research: Atmospheres*, 123, 5720–5738. <https://doi.org/10.1029/2017JD027563>, 2018.
- Fuhlbrügge, S., Quack, B., Tegtmeier, S., Atlas, E., Hepach, H., Shi, Q., Raimund, S., and Krüger, K.: *The contribution of oceanic halocarbons to marine and free tropospheric air over the tropical West Pacific*, *Atmos. Chem. Phys.*, 16, 7569–7585, <https://doi.org/10.5194/acp-16-7569-2016>, 2016.
- Hossaini, R., Chipperfield, M. P., Monge-Sanz, B. M., Richards, N. A. D., Atlas, E., and Blake, D. R.: *Bromoform and dibromomethane in the tropics: a 3-D model study of chemistry and transport*, *Atmos. Chem. Phys.*, 10, 719–735, <https://doi.org/10.5194/acp-10-719-2010>, 2010.
- Lal, S., Venkataramani, S., Chandra, N., Cooper, O. R., Brioude, J., and Naja, M.: *Transport effects on the vertical distribution of tropospheric ozone over western India*, *J. Geophys. Res. Atmos.*, 119, 10,012–10,026, doi:10.1002/2014JD021854, 2014.
- Lelieveld, J. et al.: *The South Asian monsoon – pollution pump and purifier*. *Science* 361, 270–273, doi:10.1126/science.aar2501, 2018.
- Li, L., A.J. Dolman, and Z. Xu: *Atmospheric Moisture Sources, Paths, and the Quantitative Importance to the Eastern Asian Monsoon Region*. *J. Hydrometeor.*, 17, 637–649, <https://doi.org/10.1175/JHM-D-15-0082.1>, 2016.
- Vogel, B., Müller, R., Günther, G., Spang, R., Hanumanthu, S., Li, D., Riese, M., and Stiller, G. P.: *Lagrangian simulations of the transport of young air masses to the top of the Asian monsoon anticyclone and into the tropical pipe*, *Atmos. Chem. Phys.*, 19, 6007–6034, <https://doi.org/10.5194/acp-19-6007-2019>, 2019.

Anonymous Referee #2

The manuscript presents a study of the transport of CHBr_3 and CH_2Br_2 , concentrating on how this might have changed over the past decades. They use a now widely-used static global sea-surface concentration field for these species, then calculate monthly fluxes based using offline meteorology. This is run through a Lagrangian model using emissions on a monthly basis. This is an area of study that is of interest to a wide audience and is appropriate in scope for ACP.

We thank Referee 1 for his/her valuable comments. We have changed the manuscript according to the comments listed below and think that these changes have improved the quality of the manuscript.

I can understand that the approach described here could yield information about the source gas delivered to the TTL/UTLS, however, I am not convinced that it is an appropriate methodology for understanding product gases. A largely expanded discussion of uncertainty is needed, as well as comparisons with product gases or referencing of this work elsewhere. The comparisons with inorganic bromine constraints could provide evidence to the argument that this methodology can give valid insights into product gas delivery to the stratosphere. Clearer and more detailed explanations are needed for this approach, as these kinds of studies have more often used models with online chemistry with the online process (e.g. photolysis, deposition, heterogeneous chemistry) and are run at higher temporal resolution.

We have added a detailed discussion of our product gas modelling approach explaining the wet deposition within FLEXPART and how the inorganic Br_y partitioning takes short-term variations into account. We also added a discussion on the uncertainties of product gas entrainment in modelling and observations. In table 2 we have added observed PG concentrations from ATTREX aircraft measurements in the West Pacific (e.g., Wales et al., 2018).

The approach to comparisons with the aircraft needs to be improved, both in presentation and approach. Comparisons of the entire observational period or simply a daily mean are insufficient. Comparisons with aircraft data have been done to a higher standard in the literature for many years. Comparisons should at least be made for the same location and time. Why was not a higher model timestamp chosen? The comments that the high concentrations are transient and not captured by models doesn't seem particularly novel, and also likely to be highly sensitive to this.

We have improved our model-measurement comparisons by sampling the model output at the measurement time and location for comparisons in Figures 4 and 7. The modelling time step is 30 min and for the campaign periods model output has been saved at this resolution. The new comparison shows slightly different results; however, the overall findings do not change substantially.

A more general point is that there must be a point at which the limitations from having a single static ocean-surface concentration dataset becomes a limiting factor in what science can be done. Are seasonally resolved predictions really possible without some exploration of the effect of seasonality in the initial concentrations? An opportunity seems to have been missed here to study the impact of perturbing this source of uncertainty.

We agree that the static ocean surface concentrations are currently a limiting factor for assessing the impact of oceanic halocarbons on the stratospheric VSLs entrainment. We have added a discussion of this limiting factor to our manuscript. A recent study from Fiehn et al. (2018) has started to investigate the potential impact of seasonally resolved emissions for the Indian ocean region. While such studies provide valuable insight into potential advantages of using seasonally resolved inventories, it is important to notice that they also have some disadvantages. Fiehn et al. used ocean biogeochemical model simulations to derive the seasonal changes, which did not include production from macro algae, but only phytoplankton sources. Given the limited spatial and temporal coverage of the available measurements, it is currently not possible to derive observation-based seasonally resolved emission inventories.

The language used throughout the manuscript could often be improved. Standard manuscript preparation rules are not followed (e.g. abstract starting with some context for the work). The text requires updating and proofreading for grammar and clarity of language.

We have improved the quality of the manuscript by following standard manuscript preparation rules such as starting the abstract with some context of the work. We have also corrected the manuscript for typos and unclear phrases and sentences.

I cannot recommend publication of this manuscript in ACP without substantial updates as highlighted above and detailed below.

Specific comments

~Pg. 1 - Please include the word “past” or “historical” in the title and relevant points in the text. This means that the readers will more easily understand how the paper’s variability fits with other recent work in the literature, including from the same authors (e.g. Ziska et al 2017).

As suggested, we have added the word ‘past’ to the title. Furthermore, we have added ‘past’ or the phrase ‘for the time period 1979-2013’ to the abstract and text.

~Pg. 2 Ln 3 - Please start the abstract with context and motivated the work, rather than straight away stating what has been done here.

We have improved the abstract by adding some context and motivation as suggested.

~Pg. 2 Ln 4 - What is meant here by “available observational datasets”? Do the authors mean all observational datasets have been used, if not which ones and why?

Thanks for pointing this out. We have used all freely available aircraft campaign data that we have been aware of. However, we can see how this phrase is confusing and have changed it to “observational data sets”.

~Pg. 3 Ln 21 - Why is the word “currently” used here when papers from 2006/2011 are cited. The authors are correct to point out that the heterogeneous chemistry and cycling of bromine has seen notable study recent. Please update this section based on recent literature (e.g. Fernandez et al 2014, Schmidt et al 2016 etc etc)

Thanks for pointing this out. We have updated the references used here based on recent literature.

~Pg. 5 Lns 16 - As before. Please clarify what is meant by “available observational data sets”.

We have changed the phrase to ‘available observational data sets derived during upper TTL aircraft campaigns ...’.

~Pg.5 Lns 17 - The use of the terms “high-resolution” to describe 1x1 modelling is odd. This is not enough to really resolve the coastal regions that huge gradients in emissions of the species studied here are seen. Global models are now regularly being run at higher resolutions, such as at horizontal resolution 12x12 km (e.g. Hu et al 2018).

We have changed the phrase to ‘Lagrangian model simulations’. The trajectory simulations are done at a higher resolution than 1°x1° with around 20 million trajectories after the spin up phase. It is true however, that the high-resolution model simulations are limited by the resolution of the meteorological input data given on a 1°x1°.

~Pg. 6 Lns 3-4 - please include the word “static” to ensure the reader is aware that no temporal information is present in the concentrations. This is mentioned later in this section, but should be said at the beginning too.

We have changed the sentence to ‘Static global surface concentration maps of the two compounds were generated from atmospheric and oceanic surface ship-borne in-situ measurements collected within the HalOcAt ...’.

~Pg. 6 Lns 12-13 - The gap-filled dataset is therefore 6 years old? Have any measurements been made since that point? Specifically, in locations where effectively no observations are present (e.g. Indian ocean). Would these observations decrease uncertainties within the dataset? What are the uncertainties within the dataset for these regions? Would this mean there is enough data to get a seasonally-resolved dataset?

A recent update of the bottom-up CHBr_3 and CH_2Br_2 Ziska et al emission estimates has been provided by Fiehn et al. (2018) after the here presented Lagrangian simulations had been finished. The update shows enhanced emissions in the tropical Indian Ocean and subtropical northern Atlantic by taking new oceanic cruises (Fiehn et al., 2017; Hepach et al., 2016) into account. Globally, the updated emissions are around 10% and 13% larger than existing observation-based estimates for CHBr_3 and CH_2Br_2 , respectively. We have added a short discussion of the new available data to section 3 pointing out possible consequences for stratospheric entrainment. Given the limited spatial and temporal coverage of the updated observational data set it is not possible to derive seasonally resolved emission inventories.

~Pg. 8 Ln 10-12. Please add a brief discussion of the lifetimes of these species to the introduction. Also state here why the different run periods were used.

We have added information on the atmospheric lifetimes of both gases to the introduction. This information is also given in the section describing the simulation of the chemical decay in FLEXPART. In order to analyse the spatial-temporal variability of stratospheric CHBr_3 injections a longer run-time was used. This information has been added to the manuscript.

~Pg. 8 Ln 16. Why is the model run period outside the observational constraint of the emissions (stated as 1989-2011 in the text)? This should be stated in the text.

As we are interested in long-term variations and trends of CHBr_3 transport and stratospheric injection, we used a longer model run period than the observational constraint period. We have extended the Ziska et al. (2013) approach by assuming constant CHBr_3 concentration fields over the full 1979-2013 time period and calculated the emission fields based on ERA-Interim data over this time period. This information has been added to the manuscript.

~Pg. 9 Lns 6-8 - What about in FLEXPART? Does this reproduce what is seen in TOMCAT? Even with the differences in timestep and online processing?

Yes, the shape of the CHBr_3 and CH_2Br_2 profiles (mainly determined by atmospheric lifetimes and transport) are very similar in TOMCAT and FLEXPART simulations, see Figure 1e and 1f in Hossaini et al. (2012) and Figure 12 in our manuscript. Absolute values are slightly different given the different emission scenarios used.

~Pg. 9 Lns 9-10 - What “photochemical” loss? Do the authors mean the prescribed loss terms they have used? What about loss through oxidation (e.g. OH)?

Yes, this refers to the prescribed chemical loss terms. We have added a short statement to the sentence. The chemical loss of CHBr_3 is largely driven by photolysis, while CH_2Br_2 loss is driven by oxidation (Hossaini et al., 2010, Figure 4).

~Pg. 9 Lns 11-13 - This approach to Br_y cycling and loss is much simpler than what is employed in the state-of-the-art chemical transport models. What sensitivity studies have been performed to see the sensitivity to this? This seems likely to cause large differences in the product gases delivered to the stratosphere.

We also added a general background discussion on the uncertainties of product gas entrainment from modelling and observations. Furthermore, we have added results from a sensitivity study showing how changes of the Br_y partitioning impact the product gas entrainment. In addition, we have added a comparison the observational data in order to discuss caveats of our offline approach.

~Pg. 9 Lns 17-23 (I) - These authors have not convinced the reader that the partial use of offline partitioning is appropriate. The lifetimes of some of these inorganic species are of the order of minutes and partitioning dramatically changes from day to night. Why too are partitioning calculations being used from 10-15 years ago, have the values predicted by the field not changed? What are the differences between the simulations of inorganic bromine in these simulations and those (even in the same model) in more recent work (e.g. in CAM-Chem, GEOS-Chem, and TOMCAT)? Either strong evidence that the answer is insensitive to this simplification needs to be added, or the discussion of product gases should be removed.

The 3-dimensional Br_y field from p-TOMCAT and its partitioning into HOBr, HBr, Br, BrO, BrONO₂, and Br₂ are given with a temporal resolution of 30 min. As the partitioning of the Br_y field varies strongly with location and time, we apply it in a first step to every air parcel according to its location each time before the wet deposition is initiated. In a second step, wet deposition is calculated individually for each inorganic bromine species based on its solubility specified by the effective Henry's law coefficient. Once wet deposition is initiated the Br_y fraction determined to be washed out is removed completely. This information has been added together with further details to the manuscript.

The simulations are not insensitive to the specific partitioning used in the study in the same way that online chemistry simulations can result in different wash-out rates. Our citation of the Yang et al. (2005) is misleading. We use a chemical partitioning derived from p-TOMCAT runs from 2012 which are based on the known homogeneous bromine chemistry and include heterogeneous reactions on aerosols (reactivating bromine radicals from the reservoir species) and we have added the relevant Yang et al. (2010) citation. We apply the partitioning every 30 min in order to take into account the high variability and day-night differences. Uncertainties in the modelled wet deposition arise from the parameterization of solubility via the effective Henry's law coefficient and from uncertainties in the Br_y partitioning caused by errors in the aerosols loading and in the mechanism used for heterogeneous reactions. Clouds and aerosols within p-TOMCAT are not matched with those in FLEXPART which might lead to an additional error source. A short discussion has been added to the manuscript.

~Pg. 9 Lns 17-23 (II) - Please give a statement here about how the model has been evaluated against the observations for inorganic bromine (like a similar statement for the VSLS on Pg. 8 Ln 30-32). Multiple recent studies have reported these observations (e.g. Koenig et al 2017)

We have added a table to the manuscript which compares VSLS source and product gases derived from measurements of the ATTREX and CONTRAST campaigns to estimates derived from the FLEXPART model simulations. The comparison for the West Pacific region shows good agreement for both, SG and PG entrainment. Note that the Br_y derived from measurements is based on BrO measurements and chemical box model simulations.

~Pg. 9 Lns 17-23 (III) - More explanation needs to be given of how the mixture of the online and offline process are considered here? There is a prescribed lifetime, does this just include photolysis or oxidation too? But it doesn't include wet deposition? Or are depositional losses being double-counted here?

The prescribed lifetime of $CHBr_3$ and CH_2Br_2 includes photolysis and oxidation but no depositional loss. The washout is only applied to the inorganic Br_y . A more detailed explanation has been added to the manuscript.

~Pg. 9 Lns 25-36 - Why not diagnosis the tropopause from the ECMWF met fields? This seems like an unnecessary simplification.

We used the cold point tropopause diagnosed from the ECMWF fields, which was calculated within the FLEXPART routine. We have added this information to the sentence.

~Pg. 10 Lns 3-5 The authors are right to point out this large uncertainty on their prediction of product bromine. However, a full discussion of this is essentially missing from the manuscript and must be added.

We have added a more detailed discussion of product gas entrainment based on our sensitivity studies and based on the comparison to the measurement derived Br_y estimates. The fact that source and product gas entrainment of $CHBr_3$ and CH_2Br_2 agree relatively well with currently available measurement-based estimates and with other model estimates indicates that the simplifications applied in our modelling approach (lifetimes of both gases and Br_y partitioning) are consistent with the current state of knowledge.

~Pg. 17 Lns 1-11 What other model-observation comparisons have been done in the literature. Have these failed or succeed in capturing the observations? Please add this information to give context for the work.

According to the best of our knowledge there is no model evaluation or comparison that has used the ACCENT data.

~Figure 2 - Why do units of concentration presented in Fig 2d in have a time dimension?

Thanks for pointing this out. We have corrected the units in Fig. 2d.

~Figure 3 - Please explain the noisy pattern seen in the model values underlayed.

The spotty features in the model simulations are a result of the high oceanic sources directly underneath interacting with localized convective transport. The latter brings localized air masses with very high bromoform mixing ratios from the boundary layer into the 15-17 km layer. We have added this explanation to the manuscript.

~Figure 4 - This figure does not clearly convey information. Why are whole campaigns solely represented as stars? Why not show some level of variability seen by both the modelling and observations? It seems like a simple box and whisker comparison would convey more information here. Why two are the multiple horizontal lines, is this a split y axis? If so please show this with an axis break symbol.

We have improved the figure by including the measurement variability and by adding an axis break symbol. Furthermore, we have improved our model-measurement comparisons by sampling the model output at the measurement time and location.

~Figure 7 - Please show uncertainties or ranges for the observations from ATTREX on the leftmost and rightmost subplots. Also, the paradigm for plotting in atmospheric science is usually that observations are shown in black and model. Please update this plot and anywhere else in the manuscript to avoid confusing readers.

We have improved the figure by including the ATTREX measurement variability and by showing the observations in black. Furthermore, we have improved our model-measurement comparisons by sampling the model output at the measurement time and location.

~Figure 8. (e) Please explain discontinuity seen at latitudes of -5 degrees N and 5 degrees N in the Indian ocean. These do not seem physically plausible.

These discontinuities result from the emission inventory which shows similar patterns in the same region. We have added a figure of the seasonal emissions to the supplement.

~Pg. 37 Ln 1 - Are only the bromoform emissions archived? What about the dibromomethane, where is this data archived?

Thanks for pointing this out. The dibromomethane data is also archived and we have updated to manuscript accordingly.

Technical comments

~Pg. 2 Ln 22 - expand “Br/dec” to include “decade”.

We have changed the manuscript accordingly.

~Pg. 5 Ln 5 - Typo - “meteorological”

We have corrected the typo.

~Pg. 5 - Ln 23-24 - Sentence does not scan well. Please rephrase. “The question if such hotspots are mainly driven by oceanic or by atmospheric processes will be answered based on the Lagrangian simulations.”

We have changed the sentence to “We will investigate if such hotspots are mainly driven by oceanic or by atmospheric processes by analysing emission patterns and transport pathways derived from the Lagrangian simulations.”

~Pg. 8 Lns 4-7 - Please update the sentence as below for readability. The sentence structure here and elsewhere could be more concise. From “with the Lagrangian particle dispersion model FLEXPART (Stohl et al., 2005) 7 Version 9.2 beta.” To: From “with the FLEXPART Lagrangian particle dispersion model (Version 9.2 beta; Stohl et al., 2005).”

We have changed the sentence as suggested.

~Pg. 11 Lns 25-27 - “In the following,” is verbose and should be removed.

We have removed the phrase.

~Pg. 35 Ln 18 - Add spaces between numbers and units here and elsewhere in the manuscript. Please refer to NIST guidance on this (<https://physics.nist.gov/cuu/Units/checklist.html>).

We have added the missing spaces between numbers and units.

~Pg. 11 Ln 25 - Both analyze and analyse are used in multiple places in the text. Please choose to use either the American or British version.

We have changed the manuscript and use the British version.

Refs.

Fernandez, R. P., Salawitch, R. J., Kinnison, D. E., Lamarque, J.-F., and Saiz-Lopez, A.: Bromine partitioning in the tropical tropopause layer: implications for stratospheric injection, *Atmos. Chem. Phys.*, 14, 13391-13410, <https://doi.org/10.5194/acp-14-13391-2014>, 2014.

Hu, L., Keller, C. A., Long, M. S., Sherwen, T., Auer, B., Da Silva, A., Nielsen, J. E., Pawson, S., Thompson, M. A., Trayanov, A. L., Travis, K. R., Grange, S. K., Evans, M. J., and Jacob, D. J.: Global simulation of tropospheric chemistry at 12.5 km resolution: performance and evaluation of the GEOS-Chem chemical module (v10-1) within the NASA GEOS Earth system model (GEOS-5 ESM), *Geosci. Model Dev.*, 11, 4603- 4620, <https://doi.org/10.5194/gmd-11-4603-2018>, 2018.

Koenig, T. K. et al. : BrO and inferred Bry profiles over the western Pacific: relevance of inorganic bromine sources and a Bry minimum in the aged tropical tropopause layer, *Atmos. Chem. Phys.*, 17, 15245-15270, <https://doi.org/10.5194/acp-17-15245-2017>, 2017.

Schmidt, J. A., et al. (2016), Modeling the observed tropospheric BrO background: Importance of multiphase chemistry and implications for ozone, OH, and mercury, *J. Geophys. Res. Atmos.*, 121, doi:10.1002/2015JD024229.

Ziska, Franziska, et al. "Future emissions of marine halogenated very-short lived substances under climate change." *Journal of Atmospheric Chemistry* 74.2 (2017): 245- 260.

References

Fiehn, A. et al. Delivery of halogenated very short-lived substances from the west Indian Ocean to the stratosphere during the Asian summer monsoon. Atmos. Chem. Phys. 17, 6723–6741, 2017.

Fiehn, A., Quack, B., Stemmler, I., Ziska, F. & Krüger, K. Importance of seasonally resolved oceanic emissions for bromoform delivery from the tropical Indian Ocean and west Pacific to the stratosphere. Atmos. Chem. Phys. 18, 11973–11990, 2018.

Hepach, H. et al. Biogenic halocarbons from the Peruvian upwelling region as tropospheric halogen source. Atmos. Chem. Phys. 16, 12219–12237, 2016.

Hossaini, R., Chipperfield, M. P., Monge-Sanz, B. M., Richards, N. A. D., Atlas, E., and Blake, D. R.: Bromoform and dibromomethane in the tropics: a 3-D model study of chemistry and transport, Atmos. Chem. Phys., 10, 719-735, <https://doi.org/10.5194/acp-10-719-2010>, 2010.

Hossaini, R., Chipperfield, M. P., Feng, W., Breider, T. J., Atlas, E., Montzka, S. A., Miller, B. R., Moore, F. and Elkins, J.: The contribution of natural and anthropogenic very short-lived species to stratospheric bromine, Atmospheric Chemistry and Physics, 12(1), 371–380, doi:10.5194/acp-12-371-2012, 2012.

Wales, P. A., Salawitch, R. J., Nicely, J. M. Anderson, D. C., Canty, T. P., Baidar, S., et al., Stratospheric injection of brominated very short-lived substances: Aircraft observations in the Western Pacific and representation in global models. Journal of Geophysical Research: Atmospheres, 123. <https://doi.org/10.1029/2017JD027978>, 2018.

Yang, X., Cox, R. A., Warwick, N. J., Pyle, J. A., Carver, G. D., O'Connor, F. M., and Savage, N. H.: Tropospheric bromine chemistry and its impacts on ozone: A model study, J. Geophys. Res., 110, D23311, doi:10.1029/2005JD006244, 2005.

Yang, X., Pyle, J. A., Cox, R. A., Theys, N., and Van Roozendael, M.: Snow-sourced bromine and its implications for polar tropospheric ozone, Atmos. Chem. Phys., 10, 7763-7773, doi:10.5194/acp-10-7763-2010, 2010.

Variability and **past** long-term changes of brominated VSLS at the tropical tropopause

Susann Tegtmeier^{1*}, Elliot Atlas², Birgit Quack¹, Franziska Ziska¹, and Kirstin Krüger³

¹GEOMAR Helmholtz Centre for Ocean Research Kiel, Kiel, Germany

*Now at: Institute of Space and Atmospheric Studies, University of Saskatchewan, Saskatoon, Canada

²Rosenstiel School of Marine and Atmospheric Science, University of Miami, Miami, Florida, USA

³Meteorology and Oceanography Section, Department of Geosciences, University of Oslo, Oslo, Norway

Abstract

Halogenated very short-lived substances (VSLS), such as bromoform (CHBr₃), can be transported to the stratosphere and contribute to the halogen loading and ozone depletion. Given their highly variable emission rates and their short atmospheric lifetimes, the exact amount as well as the tempo-spatial variability of their contribution to the stratospheric halogen loading is still uncertain. We combine ~~available~~ observational data sets with Lagrangian atmospheric modelling in order to **analyse** ~~analyze~~ the spatial and temporal variability of the CHBr₃ injection into the stratosphere **for the time period 1979-2013**. Regional maxima with mixing ratios of up to 0.4-0.5 ppt at 17 km altitude are diagnosed to be over Central America (1) and over the Maritime Continent/West Pacific (2), both of which are confirmed by high-altitude aircraft campaigns. The CHBr₃ maximum over Central America is caused by the co-occurrence of convectively driven short transport time scales and strong regional sources, which in conjunction drive the seasonality of CHBr₃ injection. Model results at a daily resolution reveal isolated, exceptionally high CHBr₃ values in this region which are confirmed by aircraft measurements during the ACCENT campaign and do not occur in spatially or temporally averaged model fields. CHBr₃ injection over the West Pacific is centred south of the equator due to strong oceanic sources underneath prescribed by the here applied bottom-up emission inventory. The globally strongest stratospheric CHBr₃ injection of up to 0.6 ppt is diagnosed to occur over the region of India, Bay of Bengal and Arabian Sea (3), however, no data from aircraft campaigns are available to confirm this finding. Interannual variability of stratospheric CHBr₃ injection of 10-20% is to a large part driven by the variability of coupled ocean-atmosphere circulation systems. Long-term changes, on the other hand, correlate with the regional SST trends resulting in positive trends of stratospheric CHBr₃ injection over the West Pacific and Asian monsoon region and negative trends over the East Pacific. For the tropical mean, these opposite regional trends balance each other out resulting in a relatively weak positive trend of 0.017 ± 0.012 ppt Br/**decade** for 1979-2013, corresponding 3% Br/**decade**. The overall contribution of CHBr₃ together with CH₂Br₂ to the stratospheric halogen loading accounts for 4.7 ppt Br, in good agreement with existing studies, with 50%/50% being injected in form of source and product gases, respectively.

1 Introduction

It has long been recognized that the depletion of stratospheric ozone over the last 30 years is mainly caused by human-made chlorine- and bromine-containing substances, often referred to as ozone-depleting substances (ODS) (Carpenter and Reimann et al., 2014). The Montreal Protocol, crafted in 1987 to control the production and consumption of ODSs, has been very successful in reducing the emission of the long-lived halocarbons. As a result, the overall abundance of ODS in the atmosphere has been decreasing since the beginning of the 21st century and the depletion of stratospheric ozone **layer** is expected to **level-off and reverse recover around the middle of the 21st century** (Austin and Butchart, 2003; Carpenter and Reimann et al., 2014, **Salawitch et al., 2019**).

In contrast to long-lived halocarbons, the so-called Very Short-Lived Substances (VSLS) with chemical lifetimes of less than 6 months (e.g. Ko and Poulet et al., 2003), are not controlled by the Montreal Protocol and are even suggested to increase in the future (e.g., Pyle et al., 2007; Tegtmeier et al., 2015; Ziska et al., 2017). Brominated VSLS are primarily of natural origin emitted by oceanic macroalgae and phytoplankton (e.g., Quack and Wallace, 2003). Over the last years there has been increasing evidence from observational (e.g., Dorf et al., 2008; Sioris et al., 2006; McLinden et al., 2010; Brinckmann et al., 2012) and modelling (e.g., Warwick et al. 2006; Liang et al., 2010; Hossaini et al., 2012b; Tegtmeier et al., 2012; **Hossaini et al., 2016**) studies that VSLS provide a significant contribution to stratospheric total bromine (Br_y). Current estimates of this contribution **are about 5 (3 - 7) ppt bromine** ~~range between 2 and 8 ppt~~ (Carpenter and Reimann et al., 2014; **Engel and Rigby, 2018**; Navarro et al., 2015; Wales et al., 2018). The injection of VSLS into the stratosphere in form of source gases (SGs) or inorganic product gases (PGs) depends strongly on the efficiency of troposphere-stratosphere transport versus the degradation of the source gases (through photochemical loss) and product gases (through wet deposition). In particular, the question of heterogeneous release of bromine back to the gas phase, which determines the efficiency of wet deposition as a sink for Br_y , is currently under discussion (e.g., Salawitch, 2006; Aschmann et al., 2011, **Fernandez et al., 2014, Schmidt et al., 2016**). Once brominated VSLS have reached the stratosphere in the form of SG or PG, they participate in ozone depletion at middle and high latitudes (Braesicke et al., 2013; Yang et al., 2014; Sinnhuber and Meul, 2015). Through their relatively large impact on

ozone in the lower stratosphere, they contribute -0.02Wm^{-2} to global radiative forcing (Hossaini et al., 2015).

The most abundant bromine containing VSLS are bromoform (CHBr_3) and dibromomethane (CH_2Br_2) **with atmospheric lifetimes estimates ranging from 16 (50) days at the ocean surface to 29 (400) days in the TTL for CHBr_3 (CH_2Br_2) (Hossaini et al., 2012b)**. Both gases have potentially important source regions in tropical, subtropical and shelf waters (e.g., Butler et al., 2007; Quack et al., 2007). The emissions of brominated VSLS from the ocean into the atmosphere can be derived based on their concentration gradient between water and air, wind speed, sea surface temperature and salinity (e.g. Nightingale et al. 2000; Quack and Wallace 2003; Ziska et al. 2013). The magnitude and distribution of brominated VSLS emissions are poorly constrained given the sparse observational data base of their oceanic and atmospheric concentrations (Ziska et al., 2013). Current emission inventories have been mostly derived via the top-down approach by adjusting the estimated VSLS emissions in a global atmospheric model to produce agreement of the model simulations with aircraft observations. For CHBr_3 , the current global top-down emissions range between 426 - 530 Gg Br/year (Liang et al., 2010; Warwick et al., 2006, Ordonez et al., 2012), while the bottom-up approach based on statistical gap filling of an observational data base suggests smaller global fluxes of 164-236 Gg Br/year (Ziska et al., 2013). A recent oceanic modelling study taking into account source and sink processes projects open ocean emissions of around 72 Gg Br/year in form of CHBr_3 , not including the strong coastal sources (Stemmler et al., 2015). Quantitative evaluations of various emission inventories demonstrated that the performance of the individual inventories depends strongly on the region and model applied for the evaluation (Hossaini et al., 2013; Hossaini et al., 2016).

Stratospheric injection of trace gases with lifetimes of days to weeks is most efficient in regions of strong, high reaching convective activity such as the West Pacific (e.g., Aschmann et al., 2009; Pisso et al., 2010; Marandino et al., 2013). The Asian monsoon represents another important pathway to the lower stratosphere (e.g., Randel et al. 2010, Tissier and Legras, 2016) entraining mostly Southeast Asian planetary boundary layer air with the potential to include emissions from the Indian Ocean and Bay of Bengal (Fiehn et al., 2017, 2018b). In both regions, the West Pacific and the Indian Ocean, these effective transport pathways may coincide with strong oceanic emissions (e.g., Ziska et al., 2013) potentially leading to anomalously large injection of brominated VSLS. While aircraft measurements in the West Pacific have confirmed

high concentrations of brominated VSLS such as CHBr_3 (Wales et al., 2018), the role of the Asian monsoon as an entrainment mechanism for VSLS is not clear due to the lack of observations in this region. Given the high variability of VSLS measurements in the tropical tropopause layer (TTL) (Liang et al., 2010), the overall distribution and temporal short- and long-term changes are not well known. Modelling the VSLS distribution in this region depends on the magnitude and distribution of prescribed oceanic emissions, on the representation of tracer transport in the models and on related uncertainties in both quantities (Hossaini et al., 2016). Reconciling snapshots of VSLS distributions derived from high resolution aircraft measurements with lower spatially and temporally smoothed global modelling fields remains a challenge.

Changes in oceanic biogeochemical systems over the last decades most likely lead to changes in the marine VSLS production. However, due to the sparse data coverage and missing process understanding, it is currently not possible to quantify such long-term changes of the oceanic halocarbon production and consequences for the air-sea flux (Ziska et al., 2017). Changes in ~~meteorological~~ **meteorological** and oceanic surface parameters, which also impact the oceanic emission strength, on the other hand, have been quantified. Based on increasing sea surface temperature, salinity and wind speed, VSLS emissions are projected to increase over the recent past (Ziska et al., 2013) and for future climate projections until 2100 (Tegtmeier et al., 2015, Ziska et al., 2017). At the same time, atmospheric transport of VSLS is driven by changes of the atmospheric circulation. In particular, changes of tropical, high reaching convection can be expected to have a large influence on the transport of VSLS from the ocean surface to the TTL (Aschmann et al., 2011; Hossaini et al., 2013). Long-term changes of VSLS injections into the stratosphere are difficult to predict as they are driven by various processes including changes in surface emissions, troposphere-stratosphere transport, and tropospheric chemistry (Pyle et al., 2007; Hossaini et al., 2012a).

In our study, we combine ~~available~~ observational data sets **derived during upper TTL aircraft campaigns**, ~~including surface and upper air measurements~~, with **Lagrangian model simulations and an observation based VSLS emission climatology** ~~high-resolution atmospheric modelling~~ in order to **analyse** ~~analyze~~ the spatial and temporal variability of VSLS injection into the stratosphere. Model simulations and data sets are introduced in Section 2. A detailed picture of the distribution of CHBr_3 in the TTL (Section 3.1) is derived from Lagrangian transport simulations applied to a bottom-up, observation-based emission

inventory. Analyses of the trajectory pathways and comparisons to aircraft observations allow us to evaluate how well we know the hotspots of CHBr_3 injection (Sections 3.2 to 3.4). **We will investigate if such hotspots are mainly driven by oceanic or by atmospheric processes by analysing emission patterns and transport pathways derived from the Lagrangian simulations.** ~~The question if such hotspots are mainly driven by oceanic or by atmospheric processes will be answered based on the Lagrangian simulations.~~ We present the first estimates of the long-term changes of CHBr_3 injection based on changing oceanic emissions and transport processes (Section 3.5). Finally, the overall contribution of CH_2Br_2 and CHBr_3 to the stratospheric bromine loading is determined from the model simulations (Section 3.6) and compared to existing studies. A summary and discussion of the key results is given in Section 4.

2 Data and Model

2.1 Global emission climatology

The global emission scenario from Ziska et al. (2013) is a bottom-up estimate of oceanic CHBr_3 , CH_2Br_2 , and CH_3I fluxes. Here we focus on the two brominated compounds. **Static** global surface concentration maps of the two compounds were generated from atmospheric and oceanic surface ship-borne in-situ measurements collected within the HalOcAt (Halocarbons in the ocean and atmosphere) database project (<https://halocat.geomar.de>). In a first step, the in-situ surface measurements were classified based on physical and biogeochemical characteristics of the ocean and atmosphere important for the CH_2Br_2 and CHBr_3 distribution and sources. In a second step, the global $1^\circ \times 1^\circ$ grid was filled by extrapolating the in-situ measurements within each classified region based on the ordinary least square and robust fit regression techniques. The method includes all in situ-measurements available through the HalOcAt data base at the time, regardless of season and year of the measurement. The resulting concentration maps are taken to represent climatological fields of a 23-year long time period covering **1979 to 2013**. Based on the global concentration maps the oceanic emissions were calculated with the transfer coefficient parameterization of Nightingale et al. (2000), which was adapted to CHBr_3 and CH_2Br_2 (Quack and Wallace, 2003). While the concentration maps do not provide any temporal variability, the emission parameterization is based on 6 hourly meteorological ERA-Interim data (Dee et al., 2011) allowing for relative emission peaks related to maxima in the horizontal

wind fields and sea surface temperature. The emission inventory is available at 6-hourly, daily, and monthly temporal resolution or as a climatology product calculated as a long-term average emission field. **Seasonal CHBr₃ emission maps averaged over 1979-2013 are shown in the supplementary material (Fig. S1).**

2.2 Aircraft campaigns

We **analyse** ~~analyze~~ the spatial and temporal variability of CHBr₃ in the TTL based on the comparison of Lagrangian transport simulations to data from aircraft campaigns. CHBr₃ measurements in the upper TTL are currently available from seven aircraft campaigns. Nearly all of the campaigns took place over Central America, except for the ATTREX campaign which was in large part conducted over the Pacific. Detailed information about the aircraft missions including location and time period are presented in Table 1.

Table 1. Aircraft campaigns with CHBr₃ measurements used in the study.

Campaign (Aircraft)	Full name	Max. altitude	Location	Time period	Database/ Reference
ACCENT (WB-57)	Atmospheric Chemistry of Combustion Emissions Near the Tropopause	19 km	Southern US Gulf of Mexico East Pacific	1999 April, September	http://espoarchive.nasa.gov/archive/browse/accent
Pre-AVE (WB-57)	Pre-Aura Validation Experiment	19 km	Southern US Gulf of Mexico East Pacific	2004 January – February	http://espoarchive.nasa.gov/archive/browse/pre_ave
AVE (WB-57)	Aura Validation Experiment	19 km	Southern US Gulf of Mexico	2005 June	https://espoarchive.nasa.gov/archive/browse/ave
CR-AVE (WB-57)	Aura Validation Experiment (Costa Rica)	19 km	Southern US Gulf of Mexico East Pacific	2006 January - February	https://espoarchive.nasa.gov/archive/browse/cr_ave

TC4 (WB-57)	Tropical Composition, Cloud and Climate Coupling	19 km	Southern US Gulf of Mexico East Pacific	2007 August	Toon et al. (2010)
SEAC4RS (ER-2)	Studies of Emissions, Atmospheric Composition, Clouds and Climate Coupling by Regional Surveys	19 km	Southern US Gulf of Mexico	2013 September	https://espo.nasa.gov/missions/seac4rs
ATTREX (Global Hawk)	Airborne Tropical TRopopause Experiment	19 km	East Pacific	2013 February - March	http://espo.nasa.gov/missions/attrex
		18 km	West Pacific	2014 February - March	

2.3 VSLs transport modelling

We are interested in the direct contribution of CHBr_3 and CH_2Br_2 to stratospheric halogen loading in the form of source and product gas contributions. Therefore, the atmospheric transport of the two compounds from the oceanic surface into the upper troposphere and TTL is simulated **with the FLEXPART Lagrangian particle dispersion model (Version 9.2 beta; Stohl et al., 2005; 2010)** ~~with the Lagrangian particle dispersion model FLEXPART (Stohl et al., 2005) Version 9.2 beta.~~ The oceanic emissions, based on the sea-to-air flux data from Ziska et al. (2013), prescribe the amount of CH_2Br_2 and CHBr_3 released in the FLEXPART simulations with each air parcel trajectory. The global sea-to-air flux, given on a $1^\circ \times 1^\circ$ grid, is used here at a monthly mean temporal resolution. For CHBr_3 , 90 trajectories are released per month from each grid box carrying the gas amount prescribed by the emission scenario. For the longer-lived CH_2Br_2 , 45 trajectories are released per month. Once all brominated SG and PG has been removed from a trajectory through chemical decay and wet deposition, the trajectory is automatically terminated, so that the number of all active trajectories stays roughly constant (~ 20 million) at all times after the initial spin-up period. The global CHBr_3 simulations are run for 35 years from 1979 to 2013 with a spin-up period of 6 months **in order to analyse in detail the spatial-temporal variability and long-term changes of stratospheric injection.** For the

longer-lived CH_2Br_2 **the spatial-temporal variability is known to be much smaller (Hossaini et al., 2010) and** runs are carried out for three years from 2011 to 2013 with a spin-up period of 18 months.

The transport in FLEXPART is driven by meteorological fields from the ECMWF (European Centre for Medium-Range Weather Forecasts) reanalysis model. FLEXPART includes parameterizations for moist convection (Forster et al., 2007) and turbulence in the boundary layer and free troposphere (Stohl and Thomson, 1999), dry deposition, and scavenging (Stohl et al., 2005). The runs are based on the 6-hourly fields of horizontal and vertical wind, temperature, specific humidity, convective precipitation, and large scale precipitation from the ECMWF reanalysis product ERA-Interim (Dee et al., 2011) given at a horizontal resolution of $1^\circ \times 1^\circ$ on 60 model levels. A pre-processor retrieves the meteorological fields from the ECMWF archive, including the vertical wind, which is calculated in hybrid coordinates mass-consistently from spectral data. FLEXPART has been validated based on comparisons with measurement data from three large-scale tracer experiments (Stohl et al., 1998) and with results from intercontinental air pollution transport studies (e.g., Forster et al., 2001; Stohl and Trickl, 1999). Previous FLEXPART studies using a similar model setup as applied here have shown a very good agreement between diagnosed and observed VSLS profiles (e.g., Tegtmeier et al., 2013; Fuhlbrügge et al., 2016).

FLEXPART includes the simulation of chemical decay by reducing the tracer mass carried by each air parcel corresponding to its prescribed chemical lifetime. We set the atmospheric lifetime of CHBr_3 (CH_2Br_2) to an altitude-dependent lifetime profile ranging from 16 (50) days at the ocean surface to 29 (400) days in the TTL (Hossaini et al., 2012b). The lifetime profiles were derived from simulations of the chemical tropospheric loss processes of CHBr_3 and CH_2Br_2 with the chemical transport model TOMCAT (Chipperfield, 2006). Previously, profiles from TOMCAT have been shown to agree well with aircraft observations in the tropical troposphere (Hossaini et al., 2012b).

The bromine resulting from the photochemical loss of CH_2Br_2 and CHBr_3 , **based on prescribed loss terms**, contributes to the inorganic product gases. In the FLEXPART simulations, these product gases are grouped together as Br_y and transported together with the VSLS source gases along the trajectory. **Thus, we assume instantaneous conversion between organic intermediate product gases and Br_y , which has been shown to be reasonable by Hossaini et al. (2010).** Br_y can be removed effectively from the troposphere through wet scavenging by

rain or ice (Yang et al., 2005). FLEXPART includes in-cloud as well as below-cloud scavenging, which is initiated if the relative humidity as calculated from meteorological input data exceeds 80% and the precipitation rate is larger than zero. In FLEXPART, the cloud scavenging ratio is used to model washout of soluble species. **The ratio is calculated within FLEXPART with the help of the effective Henry's law coefficient, H_{eff} , which describes the physical solubility of a species as well as the effects of dissociation. Among the members of the Br_y family, HBr and HOBr can be washed out while the remaining species Br, BrO, BrONO_2 , and Br_2 are not soluble. HBr has a very large acidity dissociation constant resulting in an effective Henry's law coefficient of $7.1 \times 10^{13} \text{ M/atm}$ for $T = 298 \text{ K}$ and $\text{pH} = 5$ (Yang et al., 2005). While HBr provides the main pathway for wet removal of inorganic Br_y , HOBr is also soluble due to physical solubility, but not due to dissociation (Frenzel et al., 1998) with $H_{\text{eff}} = 6.1 \times 10^3 \text{ M/atm}$. In order to determine which fractions of Br_y are in the form of HBr and HOBr, we apply the Br_y partitioning derived from p-TOMCAT simulations (Yang et al., 2010). ~~Note that the chemical scheme of p-TOMCAT includes heterogeneous reactions on aerosols which reactivate bromine radicals from the reservoir species (Yang et al., 2005; 2010). By directly using the p-TOMCAT Br_y partitioning in the FLEXPART model runs these aerosol effects have been taken into consideration when simulating the wet removal of Br_y .~~**

Based on analysed wind-fields together with complex chemical schemes p-TOMCAT simulates the tracer distribution in the troposphere and lower stratosphere including gaseous phase bromine chemistry. The 3-dimensional Br_y field from p-TOMCAT and its partitioning into HOBr, HBr, Br, BrO, BrONO_2 , and Br_2 are given at a time step of 30 min. As the partitioning of the Br_y field varies strongly with location and time, we apply it in a first step to every air parcel according to its location each time before the wet deposition is initiated. In a second step, wet deposition is calculated individually for each inorganic bromine species based on its solubility specified by the effective Henry's law coefficient, as described above. Once wet deposition is initiated the Br_y fraction determined to be washed out is removed completely.

Dissolved inorganic bromine can be released back to the gas phase by heterogeneous chemical reactions (Abbatt, 2003; Salawitch, 2006), extending the tropospheric lifetime of Br_y by altering the efficiency of wet deposition (von Glasow et al., 2004). The heterogeneous reactions on aerosols which reactivate bromine radicals from the reservoir

species (Yang et al., 2005; 2010) are included in the chemical scheme of p-TOMCAT. This release of bromine back to the gas phase results in elevated BrO/Br_y ratios (Yang et al., 2010) and thus a lower fraction of Br_y is subject to wet deposition compared to a scenario without the heterogeneous chemical reactions. As we directly use the p-TOMCAT Br_y partitioning for our trajectory simulations, these aerosol effects have indirectly been taken into account when simulating the wet removal of Br_y. Uncertainties in the modelled wet deposition arise from the parameterization of solubility via the effective Henry's law coefficient and from uncertainties in the Br_y partitioning caused by errors in the aerosols loading and in the mechanism used for heterogeneous reactions. Clouds and aerosols within p-TOMCAT are not matched with those in FLEXPART which might lead to an additional error source.

For the analysis of the spatial and temporal variability of CHBr₃ in the TTL from FLEXPART simulations and aircraft observations in Sections 3.1 to 3.5, we use mixing ratios at 17 km (approximate cold point) and mixing ratios averaged over 16-18 km (upper part of the TTL). In order to derive the amount of VSLS source and product gases entrained into the stratosphere from the model simulations in Section 3.6, we explicitly calculate the cold point along each trajectory **based on the ERA-Interim meteorological fields** as stratospheric entrainment point. The derived estimates of stratospheric VSLS entrainment depend on the meteorological input data sets and on various FLEXPART model parameters, such as the convective parameterization. The accurate representation of convection has been validated with tracer experiments and ²²²Rn measurements (Forster et al., 2007). The application of transport timescales based on vertical heating rates instead of vertical wind fields in the TTL between 15 and 17 km results in only minor differences of VSLS entrainment (Tegtmeier et al., 2012). ~~Uncertainties in the modeled wet deposition can, among others, arise from uncertainties in the Br_y partitioning prescribed by p-TOMCAT related to uncertainties in the aerosols loading and in the mechanism used for heterogeneous reactions.~~

3 Results

3.1 CHBr₃ in the TTL

Figure 1a shows the long-term annual mean CHBr₃ distribution at 17 km as derived from the Lagrangian transport calculations driven by monthly mean oceanic emission fields for the time period 1979 – 2013. Clearly, CHBr₃ has a very pronounced spatial variability due to its short lifetime. Largest CHBr₃ mixing ratios of up to 0.4 to 0.5 ppt can be found over 1) Central America, 2) the Maritime Continent and tropical West Pacific and 3) tropical Indian Ocean (all regions are highlighted by black squares in Figure 1a labelled from 1 to 3). Other tropical regions with only little convective uplift show smaller mixing ratios, mostly between 0.1 and 0.2 ppt.

Entrainment of CHBr₃ into the stratosphere shows also a large temporal variability. The seasonal variability is given here by the standard deviation over all monthly, multi-annual mean values (Figure 1b). The by far most pronounced variability is found in the region of the Asian Monsoon anticyclone, which is characterized by a strong seasonality of vertical transport processes (Randel et al., 2010). Furthermore, the distribution of CHBr₃ at the cold point over Central America shows some seasonal variations; however, of smaller magnitude. The Maritime Continent and tropical West Pacific have only a very weak seasonal cycle. Overall, the seasonal variations are more pronounced in the NH tropics and quite low in the SH tropics. **Seasonal CHBr₃ entrainment averaged over 1979-2013 are shown in the supplementary material (Fig. S2).**

Interannual variations are given in form of the standard deviation over all annual mean CHBr₃ mixing ratios at 17 km (Figure 1c). In comparison to the seasonal variability, the interannual variability is relatively small in the NH tropics, but is of similar magnitude in the SH tropics. Drivers of the seasonal and interannual variability will be discussed in the following sections. ~~In the following, we will analyze~~ **We will analyse** the three regions with maximum CHBr₃ entrainment identified above and investigate the relative importance of emissions and transport processes for the overall distribution and seasonality of stratospheric injection.

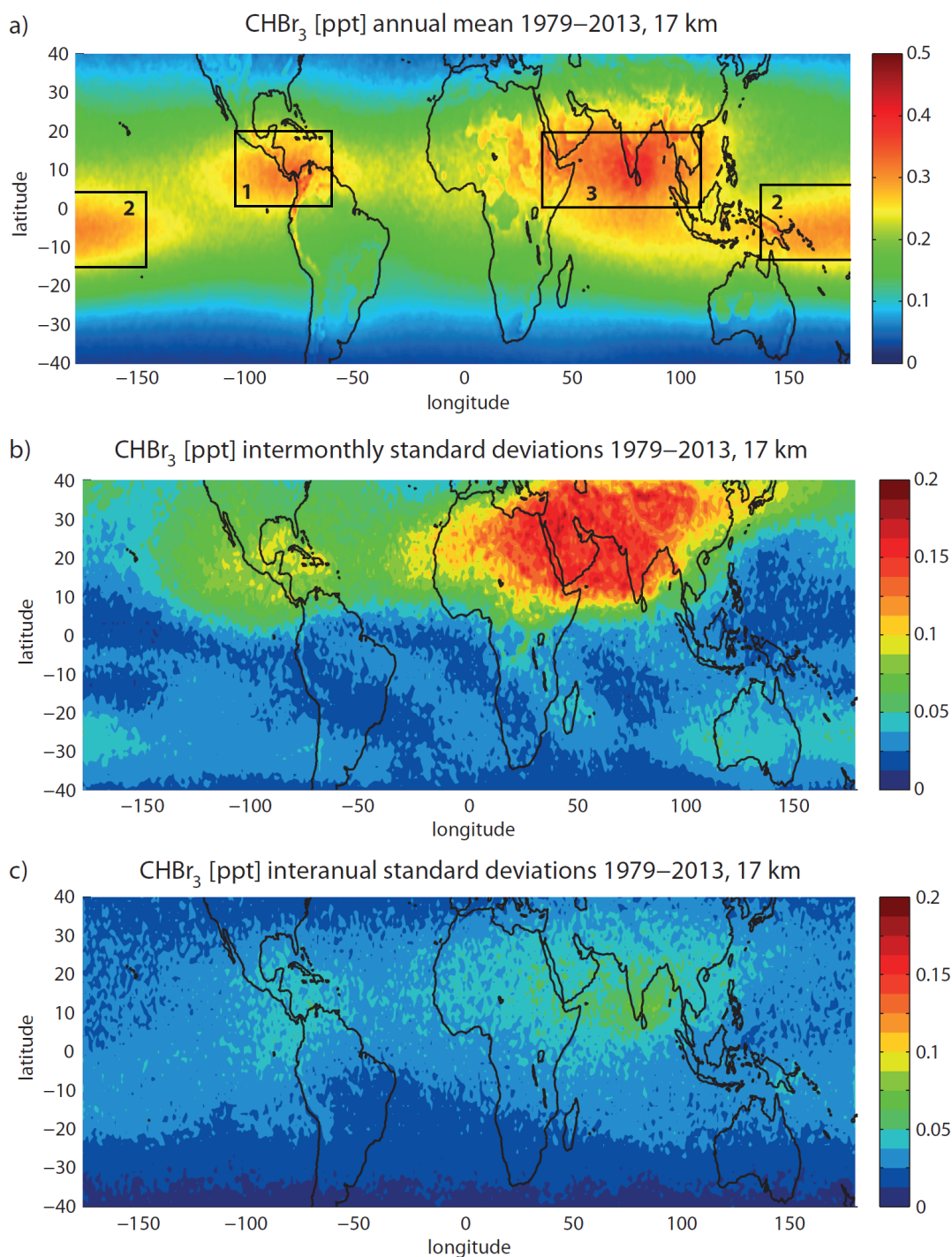


Figure 1. Modelled annual mean distribution of CHBr_3 at 17 km for 1979–2013 (a) and the inter-monthly (b) and inter-annual (c) variations given by the standard deviations over all monthly, multi-annual mean and annual mean values, respectively.

3.2 Central America

CHBr₃ in the TTL, on its way from the ocean surface to the stratosphere, shows a pronounced maximum over Central America between 0°-20°N and 60°W-110°W (black square in Figures 1a and 2a). This maximum is present all year, but most pronounced during NH summer and autumn. In the following, we will use the simulations for June/July/August to address the question, if this maximum arises from very strong oceanic sources or from strong convective transport. The impact of transport on the CHBr₃ distribution in the upper TTL is **analysed** ~~analyzed~~ by estimating the time air masses need from the ocean surface to 17 km based on the FLEXPART model simulations. The transport time of each trajectory is assigned to the location where the trajectory reaches 17 km. A map of the ‘ocean surface – 17 km transit times’ is derived by averaging over all trajectories on a 1°x1° grid. The tropical annual mean transit time is around 55 days with variations between 45 and 70 days (not shown here). Transit times over Central America for the June/July/August season are relatively short with values around 48 days (Figure 2b). However, the transit times over the East and Central Pacific are similar or even shorter, suggesting that the vertical transport in this region is as efficient as over Central America. Therefore, atmospheric transport time scales alone cannot explain the CHBr₃ maximum over Central America.

In addition to the transit time, we **analyse** ~~analyze~~ the oceanic sources of CHBr₃ over Central America. Each trajectory reaching the TTL over Central America (black square in Figure 2a) contributes a certain amount of CHBr₃ to this local maximum by carrying its prescribed oceanic emission (Ziska et al., 2013) from the surface to the cold point. The relative contribution (in %) of each trajectory is assigned to its oceanic release point, thus quantifying which ocean region contributes the largest amounts of CHBr₃ to the local maximum in the TTL. The relative contributions averaged over 1°x1° grid cells (Figure 1c) demonstrate that the largest sources stem from the Gulf of Mexico, the Caribbean Sea and the western North Atlantic. Some smaller contributions come from the west coast of North Africa and from the equatorial Atlantic. The co-occurrence of strong sources and the relatively short transport time scales over the Caribbean Sea and Central America mainly cause the local CHBr₃ maximum in the Central American TTL. While transport time scales are also short (or even shorter) in the eastern Pacific, oceanic emissions are very small there and vice versa more pronounced emissions over the Atlantic and along the coast of Africa do not cause a global maximum due to longer transport time scales.

The regional oceanic measurements in surface water, which were used to derive the extrapolated concentration and emission maps (Ziska et al., 2013), are given in Figure 2d. The available data show in particular high oceanic CHBr_3 concentrations at the Florida coastline and in the eastern part of the Gulf of Mexico. A reasonable amount of measurements with a distinctive distribution is available in this region supporting the extrapolated climatological source distribution, which leads to the CHBr_3 maximum in the TTL over Central America discussed above.

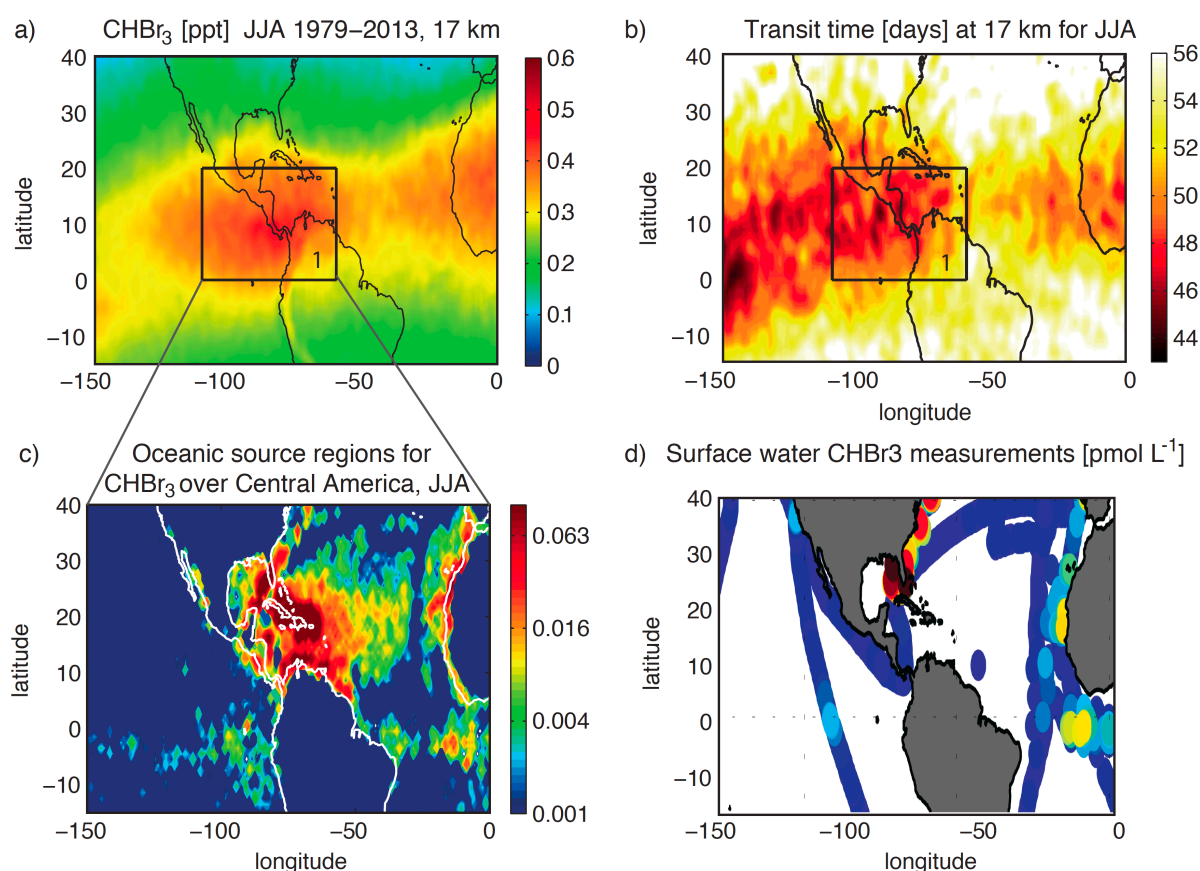


Figure 2. Modelled distribution of CHBr_3 at 17 km for JJA, 1979-2013 (a), transit time of air masses from the ocean surface to the TTL (b), oceanic source regions for CHBr_3 over Central America at 17 km given in percent per $1^\circ \times 1^\circ$ grid box (c), and measurements of oceanic CHBr_3 concentrations from the HalOcAt database used for Ziska et al. (2013) (d).

Over the last decades, the atmospheric distribution of CHBr_3 over Central America has been investigated by a number of different aircraft campaigns. We will use available upper air

measurements to evaluate the distribution and variability of the model-derived CHBr₃ fields. Details of the aircraft campaigns are given in Table 1. We show the spatial CHBr₃ distribution in the TTL as observed during three different campaigns in comparison to the model simulations (Figure 3). The altitude ranges in the upper TTL have been chosen so that each comparison includes a maximum number of observational data. While for the aircraft campaigns individual measurements are shown at the measurement locations, the model fields are averaged over the duration of the respective campaign. This method allows us to evaluate the spatial distribution of measured and modelled CHBr₃ fields, but it has the disadvantage of comparing in-situ data with temporally averaged fields. We will discuss how this can impact the comparison and how the temporal variability can be taken into account.

For the Pre-AVE campaign during Northern Hemisphere (NH) winter, CHBr₃ in the upper TTL (16-18 km) shows a latitudinal gradient with small values of 0-0.1 ppt in the northern subtropics and with higher values of up to 0.3-0.4 ppt around the equator. The same gradient is also evident from the model simulation resulting in an overall good agreement. Similarly, for the AVE campaign during NH summer, both, the observations and the model results, show a latitudinal gradient with increasing values towards lower latitudes. However, here the overall agreement is poor, since the model results are on average 50% larger than the measurements.

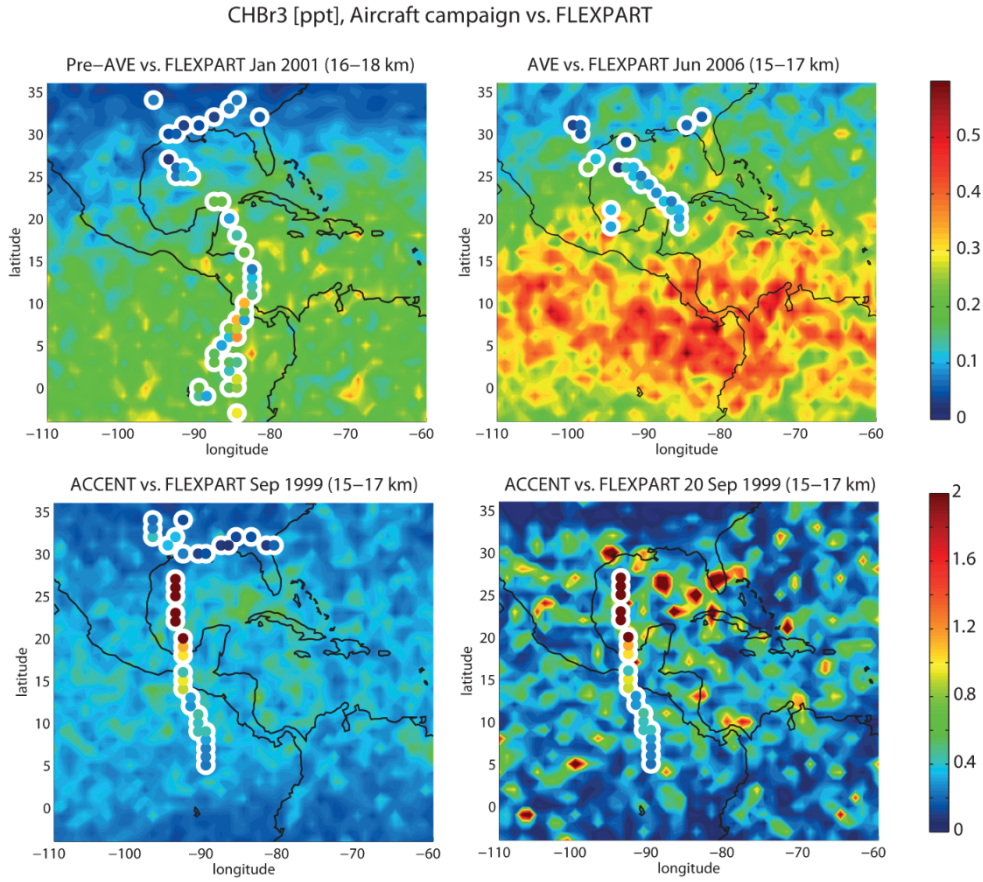


Figure 3. Modelled distribution of CHBr₃ in the upper TTL from FLEXPART (background colouring) in comparison with aircraft campaign measurements (coloured symbols with white edges). In the upper panels and lower left panel, all individual measurements from the respective campaign and the model mean over the same time period are shown. Only in the lower right panel, one individual flight (ACCENT flight from 20.09.1999) is shown with FLEXPART daily mean values to illustrate the large spatial variability including maximum values ≥ 2 ppt.

Finally, for the ACCENT campaign during NH autumn, the observations reveal extremely high CHBr₃ (up to 2 ppt) between 30°N and 20°N. While CHBr₃ is decreasing north and south of this area towards the range of 0.5-1 ppt, the values are still very high when compared to other campaigns over Central America. FLEXPART results, averaged over the time period of the ACCENT campaign (Sep 1999), show largest monthly mean CHBr₃ values of around 0.7 ppt, which are substantially smaller than the observations of 2 ppt. However, the model results look quite different and show large spatial inhomogeneities when evaluated at a daily mean resolution. Maximum model values are much higher for the daily resolution and in some locations, very close to the flight track, of similar size as the observations (around 2 ppt). **The**

spotty features in the model simulations are a result of the high oceanic sources directly underneath interacting with localized convective transport. The latter brings localized air masses with very high CHBr₃ mixing ratios from the boundary layer into the 15-17 km layer. The differences between monthly and daily mean model values make clear that CHBr₃ model-measurement comparisons may be obscured by the high variability of the field. Given this high variability and the existing uncertainties in the diagnosed oceanic sources and atmospheric transport processes, it is very difficult for a model to predict the correct in-situ values at a given time and measurement position. Nevertheless, if the large-scale emissions and transport fields are correct, spatial and temporal averaging of the model results can be expected to produce realistic mean VSLS fields and to improve the agreement with observations. Only in cases where rare events have been observed, averaging the CHBr₃ fields will not necessarily lead to a better agreement with the measurements, as demonstrated above for the ACCENT campaign. In consequence, it is important to include estimates of the spatial and temporal variability of the CHBr₃ field in all comparisons.

A summary of the CHBr₃ model results compared to all aircraft campaigns in the Central American region, taking into account ~~above-discussed~~ spatial and temporal variability, is provided in Figure 4. Here, we compare **measurements** averaged ~~calculated~~ over different parts of the flight tracks (split by latitude) with FLEXPART **coincidences** averaged over the same latitudinal bins. **In addition, the FLEXPART seasonal cycle averaged** over 110°W-80°W, the main longitudinal extent of the aircraft campaigns, **and** ~~While the campaign results refer to the respective individual years (given in Table 1), FLEXPART results are averaged over the entire campaign time period (1999-2013),~~ **is shown.** ~~In order to account for the fact that the model results are averaged over space and time, the~~ The variability of the ~~simulated~~ CHBr₃ distribution **from observations and coincident model values** is given by the standard deviation over all ~~daily-mean~~ values in the respective region. The comparison of the three campaigns during NH winter shows an overall good agreement. For some latitude bins, the modelled mean values agree very well with the observations (e.g., Pre-AVE for 5°S-15°N°), for other regions, differences of the mean values can be up to 50-100%. However, all observational mean values are within the standard deviations of the modelled field indicating good agreement of model and measurements.

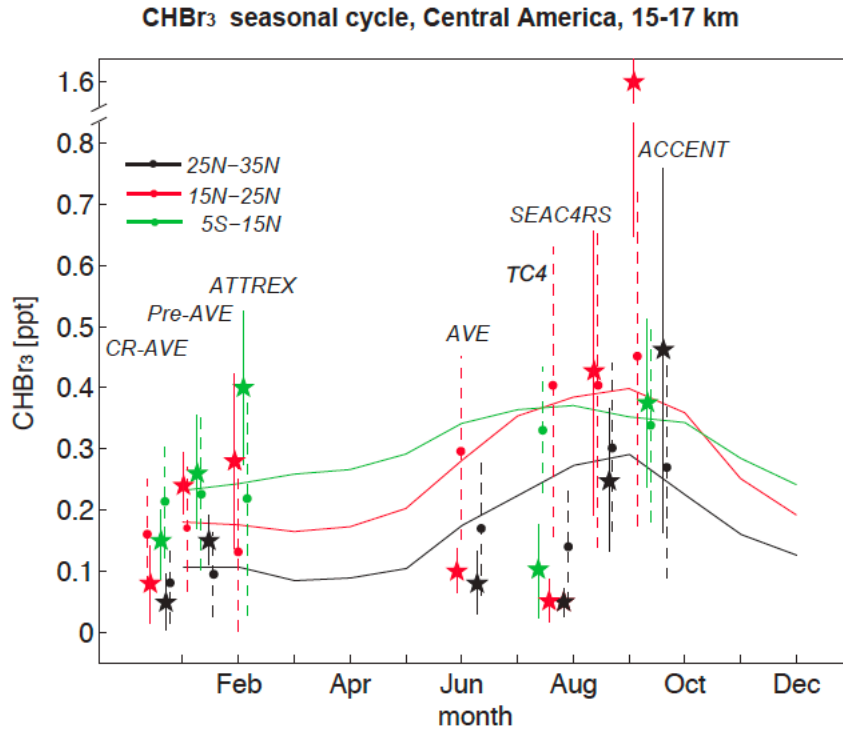


Figure 4 (new version). Seasonal cycle of CHBr₃ in the upper TTL (15-17 km) over Central America from FLEXPART simulations (dots and solid lines) in comparison with aircraft campaign measurements (stars). FLEXPART results are averaged over 110°W-80°W and 5°S-15°N (green), 15°N-25°N (red), and 25°N-35°N (black) for 1999-2013. In addition, aircraft measurements (stars) and coincident FLEXPART values (filled circles) are shown averaged over the same latitude bins and corresponding to the respective year of the campaign. The FLEXPART seasonal cycle is taken over the time period 1999 to 2013. Temporal and spatial variability of average measurements (solid vertical lines) and coincident model values (dashed vertical lines) is shown in form of the 1-sigma standard deviations over all values in the respective bin and time period as dashed vertical lines.

For the campaigns during NH summer, mean differences are in general larger than during NH winter in most cases. At the same time, the temporal and spatial variability of the simulated and observed CHBr₃ distribution is also larger so that nearly all most observations agree with the coincident model values fall within their simulated uncertainties. The large differences between the individual campaigns during NH summer confirm the increased variability suggested by the model results. For three two of the campaigns (AVE and TC4), FLEXPART overestimates the CHBr₃ values during this time of the year, while for the last other two campaigns (SEAC4RS and ACCENT), the observations and modelled values agree

relatively well except for one outlier. ~~are smaller.~~ Particularly high CHBr₃ exists for the 15°N-25°N region, observed during the ACCENT campaign at the top altitude of a plume extending from 14 – 16 km near Houston, Texas. This value is larger than the model mean, **although observational and model uncertainties slightly overlap.** ~~and also outside of the given variability range. As discussed earlier, the model results also include such high values on a daily mean basis, but only in rare occasions, suggesting that during the ACCENT campaign extraordinary atmospheric conditions with very effective convection were observed.~~ **In total, observations and model agree reasonably well with a larger variability during the NH summer and early autumn period. For this time of the year, the model also suggests a seasonal CHBr₃ maximum which is confirmed by measurements from SEAC4RS and ACCENT, but not by the AVE and TC4 campaigns.**

CHBr₃ in the upper TTL over Central America shows pronounced seasonal variations as revealed by the comparisons to aircraft campaigns in Figure 4. The CHBr₃ seasonal cycle at 17 km shows a maximum from July to October (~0.37 ppt) and a minimum from January to April (~0.17 ppt) (Figure 5a). Such seasonal variations can be caused by variations of the oceanic emissions or the atmospheric transport times. First, we **analyse** ~~analyze~~ the seasonal cycle of CHBr₃ emissions, averaged over the source region identified earlier, which show peak emissions from April to June of up to 320 pmol m⁻² hr⁻¹. This peak in surface emissions in late spring/early summer is consistent with a peak in the TTL around 2 months later, as the mean transit time from the surface to 17 km in this region is about 55 days. Second, we **analyse** ~~analyze~~ the seasonal cycle of the transit time and find a minimum from July to October, which is also consistent with the highest CHBr₃ values in the TTL during the same time period. While the amplitude of the seasonal cycle in CHBr₃ in the TTL is around 74%, seasonal variation of the emissions and the transit time are only 36% and 15%, respectively. However, the amplitude in transit time does not directly translate into the amplitude in CHBr₃ in the TTL, given the logarithmic nature of the atmospheric lifetime of chemical compounds. Overall, the interaction of both processes, oceanic emissions and transit time, cause the pronounced seasonal cycle of CHBr₃ over Central America.

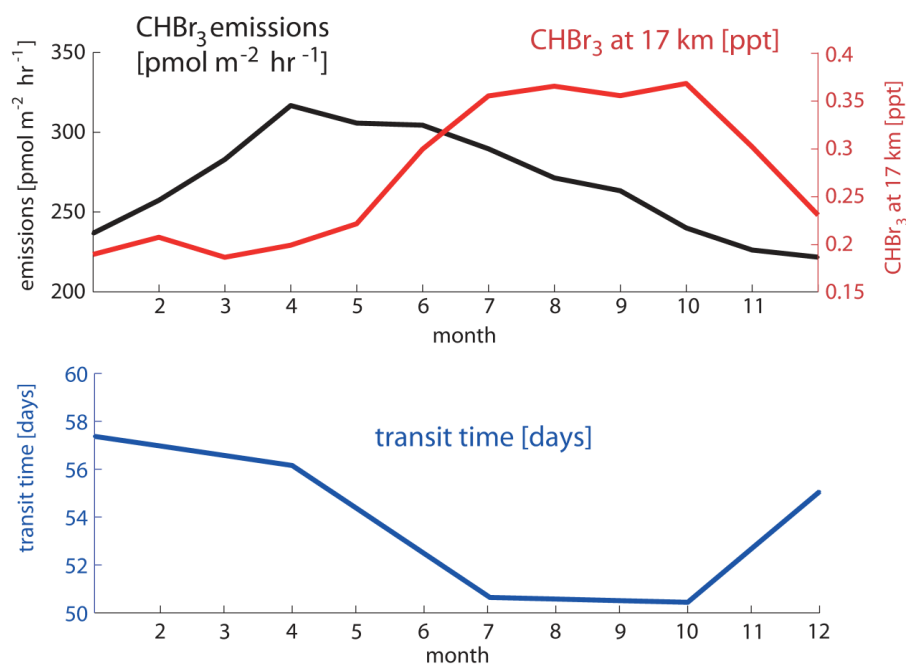


Figure 5. Seasonal cycle of CHBr₃ at 17 km over Central America (black square in Figure 2a) from FLEXPART simulations (red line), of oceanic CHBr₃ emissions averaged over the respective source region (black line) and of the ‘surface – 17 km’ mean transit time (blue line) are shown.

3.3 Maritime Continent and tropical West Pacific

CHBr₃ in the TTL shows a pronounced maximum over the Maritime Continent and tropical West Pacific between 15°S-5°N and 130°E-220°E (black square in Figures 1a and 6a). An important characteristic of this CHBr₃ maximum (referred to as the West Pacific maximum hereinafter) is that the high values are not distributed symmetrically across the equator but are shifted southwards. The maximum is present all year with no pronounced seasonal cycle (see Figure 1b). In the following, we will use annual mean results to investigate if the high values arise from very strong oceanic sources or from strong convective transport. The transit time shows smallest values of around 45 days in the West Pacific and over the Maritime continent (Figure 6b). The most important deviation from the CHBr₃ distribution at 17 km is that over the West Pacific the shortest time scales and thus most efficient transport are not centred in the Southern Hemisphere, but they are distributed symmetrically across the equator.

Oceanic sources for CHBr₃ in the West Pacific upper TTL (black square in Figure 6a) stem mostly from the Pacific Ocean, the Maritime Continent and also to a smaller degree from Central America (Figure 6c). The trajectory analysis clearly shows that the largest contribution comes from the West Pacific south of the equator, while the oceanic contributions north of the equator are lower. This pattern is directly related to the emission inventory used in this study (Ziska et al., 2013), which suggests overall stronger emissions in the southern Pacific Ocean (see Figure S1 in the supplementary material). However, available open ocean surface measurements in both, NH and SH Pacific Ocean, were sparse during the time of the construction of the inventory and mostly based on the TransBrom Sonne campaign (Krüger and Quack, 2013). The latitudinal gradient of the emission inventory with stronger emissions in the SH is based on the in-situ measurements along one cruise track from Japan to Australia during October 2009 and may not be representative for other seasons and other West Pacific regions. Future ship campaigns are necessary to confirm or improve the existing emission inventory.

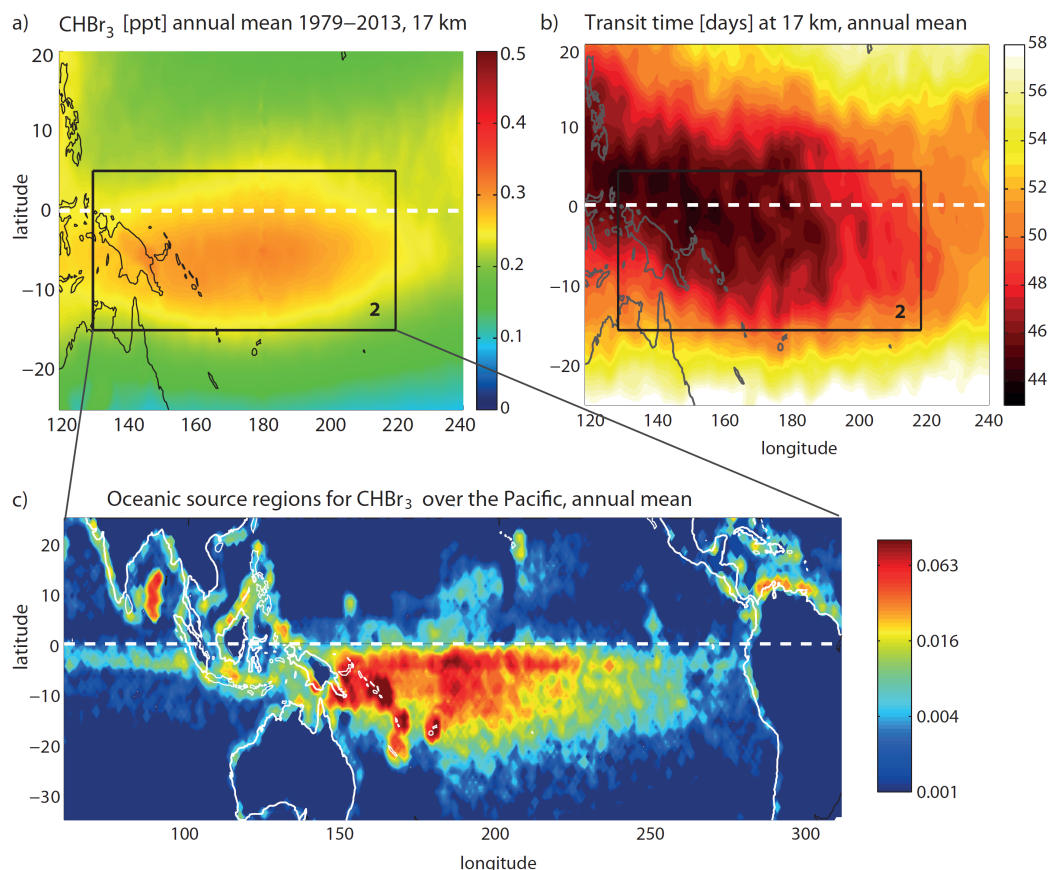


Figure 6. Modelled distribution of CHBr_3 at 17 km, annual mean 1979-2013 (a), transit time of air masses from the ocean surface to the TTL (b), oceanic source regions for West Pacific CHBr_3 at 17 km given in percent per $1^\circ \times 1^\circ$ grid box (c).

Pacific aircraft campaigns are used to further **analyse** ~~analyze~~ the hemispheric differences of the diagnosed CHBr_3 distribution. ATTREX measurements in the West Pacific in 2014 and in the East Pacific in 2013 are compared to FLEXPART simulations in Figure 7. In both regions, the comparison reveals a reasonably good agreement with increasing CHBr_3 values towards lower latitudes. **In the West Pacific, measurements and coincident model values agree best south of 10°N , while north of this the model underestimates observations by up to 0.3 ppt. In the East Pacific, model values and measurements are closer in the NH and agree mostly within their error bars. South of the equator, however, measurements are constantly larger with differences of up to 0.3 ppt. In total the modelled CHBr_3 entrainment over the Pacific is too small when compared to measurements, which could be due to an underestimation of the oceanic emissions in this region..** ~~Observations and model results agree well north of 20°N with mean values around 0.2–0.3 ppt CHBr_3 , except for one outlier in~~

the West Pacific between 25°N and 30°N. During this event, extraordinary high CHBr₃ values have been observed leading to a spike in the zonal ATTREX profile which is not reproduced by the model simulations. South of the equator, observations and model results also show a good agreement with relatively small differences of up to 25%. Between 0–20°N, however, substantial differences are found. The model results (0.2–0.3 ppt) clearly underestimate the observations (0.4–0.6 ppt) and cause differences up to 100%, at some latitudes exceeding the uncertainty range (dashed horizontal lines) given by the spatial and temporal variability of the bromoform distribution. The disagreement between model simulations and observations at these latitudes suggests, that the emissions gradient across the equator may not be a realistic phenomenon throughout the year and that larger emissions and thus also larger TTL values can be expected north of the equator.

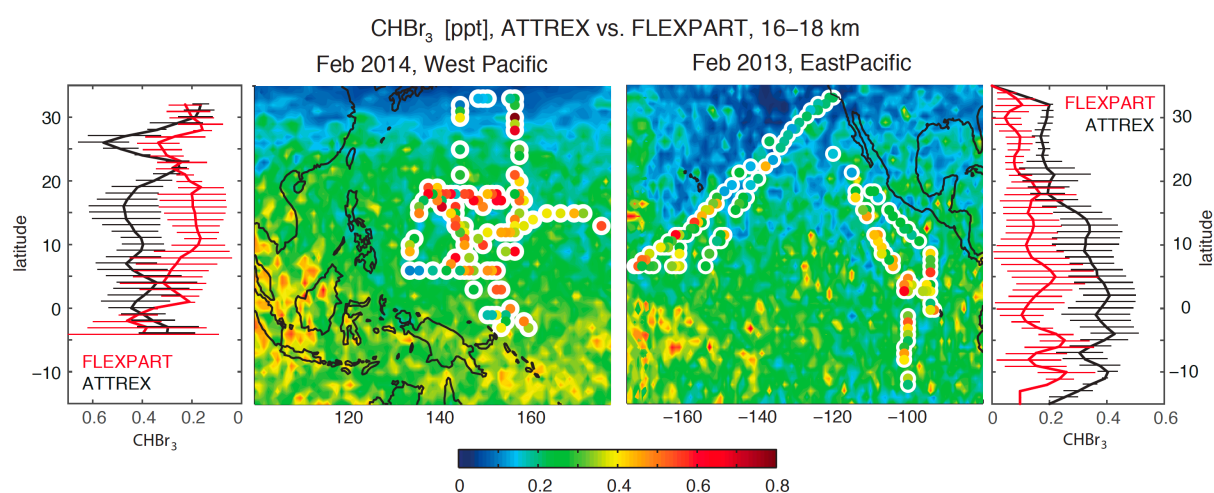


Figure 7 (new version). Modelled distribution of CHBr₃ in the uppermost TTL from FLEXPART (background colouring) in comparison with ATTREX aircraft campaign measurements (coloured symbols with white edges). Zonal means of **coincident model-measurement** comparisons are given in the leftmost panel for FLEXPART and the ATTREX campaign in February/March 2014 in the West Pacific and in the rightmost panel for FLEXPART and the ATTREX campaign in February/March 2013 in the East Pacific. **Temporal and spatial variability of measurements and coincident model values is shown in form of the 1-sigma standard deviations over all values in the respective zonal bin (horizontal lines).**

3.4 Tropical Indian Ocean

Annual mean CHBr_3 in the uppermost TTL shows a pronounced maximum over India, the Bay of Bengal and the Arabian Sea between 2°N - 22°N and 35°E - 110°E (Figures 1a, referred to as the Indian Ocean maximum hereinafter). The simulations diagnose in the long-term mean, the globally highest TTL CHBr_3 values of up to 0.5 ppt over the southern tip of India. At the same time, the intermonthly standard deviation is very high over this region (Figure 1b) due to pronounced seasonal variations. During NH summer (June/July/August), high CHBr_3 values of around 0.6 ppt are found over a large region stretching from South-East Asia all the way to North-East Africa between 10°N and 25°N . During SH summer (December/January/February), smaller maximum values of around 0.4 ppt CHBr_3 are diagnosed south of India over the Indian Ocean between 5°S - 10°N (Figure 8).

In order to evaluate the transport efficiency for oceanic short-lived trace gases in this region, the transit time is calculated from the trajectory analysis for the NH and SH summer seasons. During NH winter, transit times from the surface to the TTL show a very similar pattern as CHBr_3 in the TTL, with shortest transit times of around 45 days over the Indian Ocean coinciding with largest CHBr_3 abundance. During NH summer, on the other hand, the transit times minimize not in the region of maximum CHBr_3 abundance, but instead south of this region where air masses can reach the TTL within 43 days. Between 10°N and 25°N , the transport is still fast and the transit of short-lived species from their ocean sources will take around 48 days. Overall the transit time is similar to values found for the West Pacific and cannot solely account for the simulated maximum CHBr_3 values.

CHBr_3 contributing to the Indian Ocean TTL maximum mostly stems from the Bay of Bengal, the Arabian Sea, the equatorial region of the Indian Ocean and the coast lines of South-East Asian countries like China. Compared to the oceanic contributions identified for the Central America and West Pacific maxima, sources for the Indian Ocean CHBr_3 maxima show a large regional extent including coastal and open ocean emissions from 20°S to 30°N . Given that oceanic emissions from large parts of the Indian Ocean and adjacent coastal areas can be transported into the Asian monsoon region (Fiehn et al., 2017), the CHBr_3 maxima can be explained by the strong oceanic emissions in this region combined with efficient boundary layer–TTL transport.

The global maximum of CHBr_3 over India, Bay of Bengal and the Arabian Sea is also subject to the largest uncertainties when compared to the other maxima found in our model simulations. For the construction of the emission inventory from Ziska et al. (2013), only one data set was available for the Indian Ocean (Yamamoto et al., 2001). The data set is based on measurements at seven stations in the open ocean waters of the Bay of Bengal and reveals relatively high CHBr_3 values between 8 and 15 ng/L. Given the great distance of the sampling points from the coasts, the authors hypothesized that planktonic production is the most probable source for this high CHBr_3 abundance. Independent measurements from the OASIS campaign in 2014 confirm the subtropical and tropical West Indian Ocean as a strong source for CHBr_3 to the atmosphere, although open ocean surface concentrations were overall lower with maximum values of 8 ng/L (Fiehn et al., 2017). **A recent update of the Ziska bottom-up CHBr_3 emission climatology (Fiehn et al., 2018b) suggests enhanced emissions in the tropical Indian Ocean, which would lead to even higher stratospheric entrainment in this region.** While the high values from Yamamoto et al. (2001) were used locally for the emission climatology, the rest of the tropical Indian Ocean was filled by applying open ocean data from the tropical Atlantic and Pacific. In consequence, the emission scenario for the Indian Ocean has large uncertainties and further VLS measurements are required to confirm or improve our estimates of the Indian Ocean as the region of strongest CHBr_3 entrainment into the stratosphere.

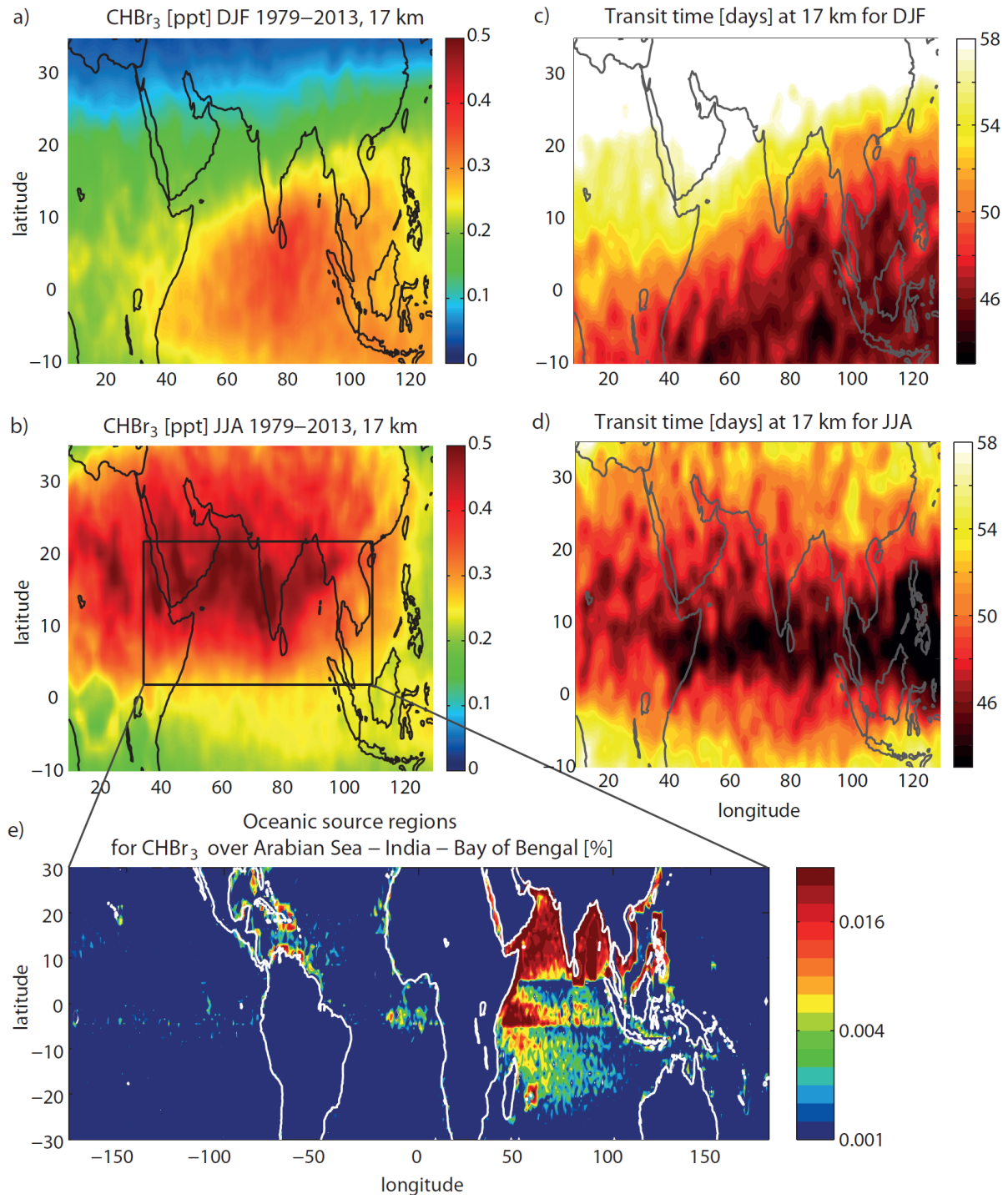


Figure 8. Modelled distribution of CHBr_3 at 17 km for DJF and JJA 1979-2013 (a, b). Transit time of air masses from the ocean surface to the TTL for DJF and JJA (c, d). Oceanic source regions for CHBr_3 over Arabian Sea, India and Bay of Bengal (black square in left uppermost panel) at 17 km given in percent per $1^\circ \times 1^\circ$ grid box (e).

3.5 Interannual and long term changes

Long term changes of tropical mean (30°N-30°S) CHBr₃ mixing ratios at 17 km show a weak but significant trend of 0.017 ± 0.012 ppt Br/**decade**, corresponding to a 10% increase of CHBr₃ over the whole time period (1979-2013). Regionally, the long term changes are more pronounced and FLEXPART simulations suggest decreasing or increasing CHBr₃ in the TTL depending on the location (Figure 9). Over South America, Australia and the Central/East Pacific, the trend is not significant given the relatively small trend values compared to the interannual variability found here. For all other regions, CHBr₃ shows a significant, positive trend of 2-10% per decade. CHBr₃ over the Indian Ocean and Maritime Continent is highlighted in Figure 9c as the region with the maximum trend (0.04 ppt Br/**decade**), mostly driven by the ENSO-related steep changes over the time period 2000-2013 (Fiehn et al., 2018a). CHBr₃ over the East Pacific is highlighted in Figure 9b as an example of a negative, but not significant trend (-0.017 ppt Br/**decade**).

The projected interannual and long-term changes of CHBr₃ injections are driven by the variability of oceanic emissions (Ziska et al., 2013), convective transport from the surface to the TTL (Aschmann et al., 2011) and transport in the TTL (Krüger et al., 2009). Our model runs are based on CHBr₃ emissions that allow for changes over time due to changing meteorological surface parameters (mostly ERA-Interim), but do not take into account oceanic biogeochemical and related CHBr₃ production changes. Due to increasing sea surface temperature and wind speed, CHBr₃ emissions increase considerably by 7.9% from 1979 to 2013 (Ziska et al., 2017). Changes in the modelled atmospheric transport are driven by long-term changes in ERA-Interim parameters such as temperature, winds and humidity fields leading to an overall trend of CHBr₃ at 17 km of 10% for 1979-2013.

The two CHBr₃ time series over the East Pacific and Indian Ocean/Maritime Continent (Figure 9b and 9c) show the opposite long-term behaviour, but also share some of the same patterns of interannual variability. In particular, signals like the steep CHBr₃ decrease from 1997/1998 to 1999, the increase from 2008 to 2009/2010 and the relatively high values in 1982 are common to both time series. We ~~analyse~~ **analyse** the common and separate drivers of the variability of the two time series further by comparing them to modes of tropical climate variability.

First, we compare the time series of stratospheric bromine in the East Pacific with the Multivariate ENSO Index (MEI; Wolter and Timlin, 2011) in Figure 9d. The irregular ENSO variations in winds and sea surface temperatures over the tropical eastern Pacific Ocean drive

changes in CHBr_3 emissions and atmospheric transport leading to a high correlation of the two time series ($r = 0.78$). During El Niño years, water in the central and eastern Pacific becomes warmer than usual and the dry and steady easterly winds turn into warm and moist westerlies leading to an increase of the oceanic emissions. This increase is driven by meteorological and oceanic surface variations but does not allow for possible changes in biogenic CHBr_3 production related to changes in the eastern Pacific upwelling system (Hepach et al., 2016). At the same time the warm East Pacific favours stronger convection intensifying the VSLs transport into the TTL (Aschmann et al., 2011). Overall, El Niño years lead to enhanced CHBr_3 injection over the East Pacific (e.g., 1982, 1986, 1991, and 1997), while La Niña corresponds to weaker CHBr_3 injection (e.g., 1988, and 2010).

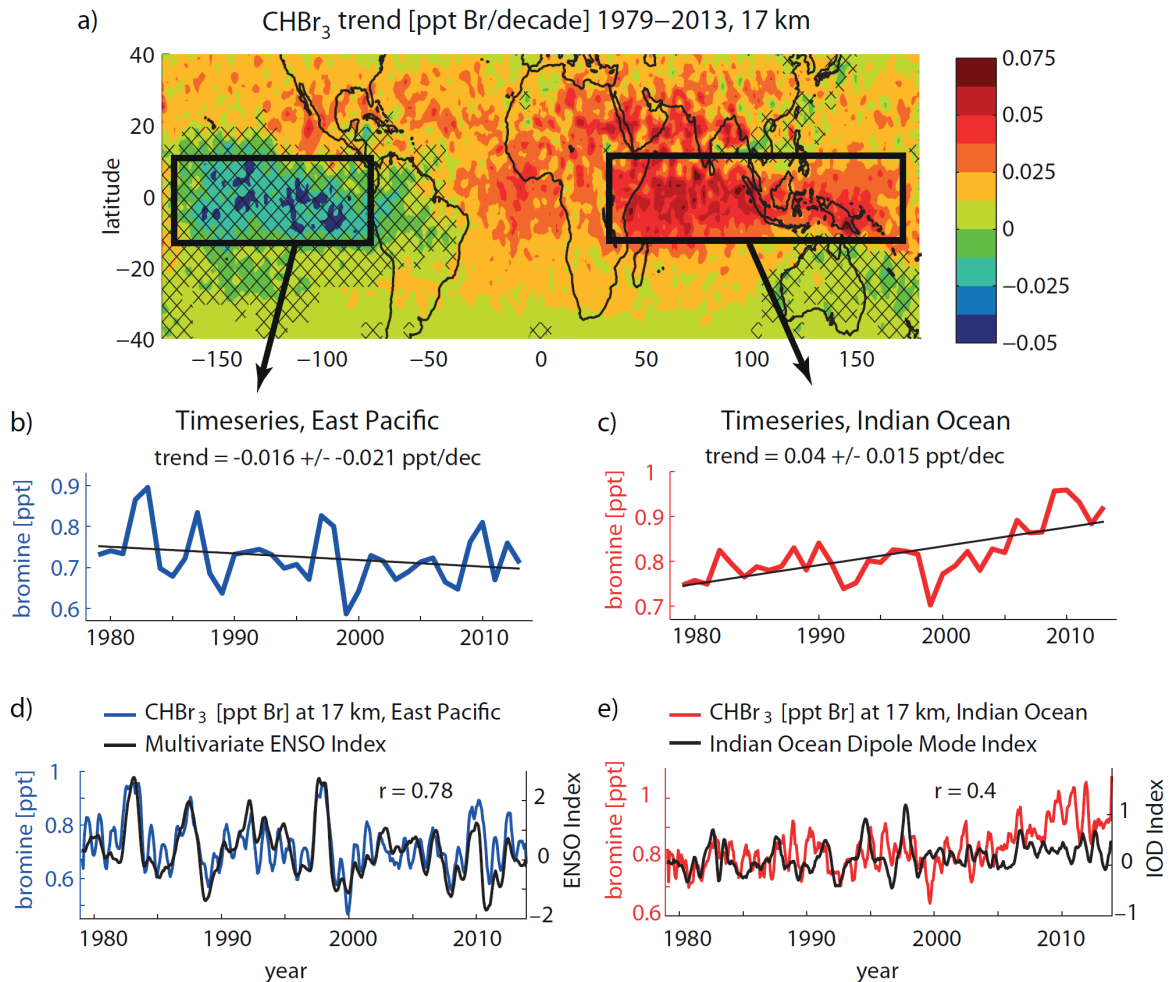


Figure 9. Modelled long-term change of CHBr_3 [Br/decade] at 17 km for the time period 1979-2013 (a). Time series (annual means) averaged over the East Pacific and the Indian Ocean/Maritime Continent/West Pacific region are shown together with the trend (b, c). Time series (5 months running mean) are shown together with the ENSO index and Indian Ocean Dipole index, respectively (d, e).

Second, variations of CHBr_3 at 17 km over the Indian Ocean and Maritime Continent are shown together with the Indian Ocean Dipole (IOD) Mode Index (Figure 9e), an indicator of the east-west temperature gradient across the tropical Indian Ocean (Saji et al., 1999). The two timeseries are weakly correlated ($r=0.4$) sharing some of their variability. The IOD is a coupled ocean-atmosphere phenomenon with anomalous cooling of the south eastern tropical Indian Ocean and anomalous warming of the western tropical Indian Ocean during a positive phase. Associated with these changes the convection normally situated over the eastern Indian Ocean warm pool shifts to the west. For some years, the positive phase results in slightly stronger CHBr_3 emissions and more effective atmospheric transport (e.g., 1982-83, 2006). In other years, strong IOD events will not impact the CHBr_3 abundance over the Indian Ocean/Maritime Continent (e.g., 1997-98). The relatively weak correlation of CHBr_3 injection and IOD results from the influence of the ENSO signal on atmospheric transport in this region. A combination of SST anomalies in the West Indian Ocean and the ENSO signal can have varying impacts on the CHBr_3 injection depending on the time of year (Fiehn et al., 2018a). While positive SST anomalies together with El Niño conditions in boreal winter and spring enhance stratospheric VSLs injection, La Niña conditions in boreal fall can also cause stronger than normal stratospheric injection. Overall, the inter-annual variability of the CHBr_3 time series is driven by a combination of the ocean-atmosphere modes in the Indian and Pacific Ocean, however, the strong increase during 2009-2013 is not related to either of the two modes.

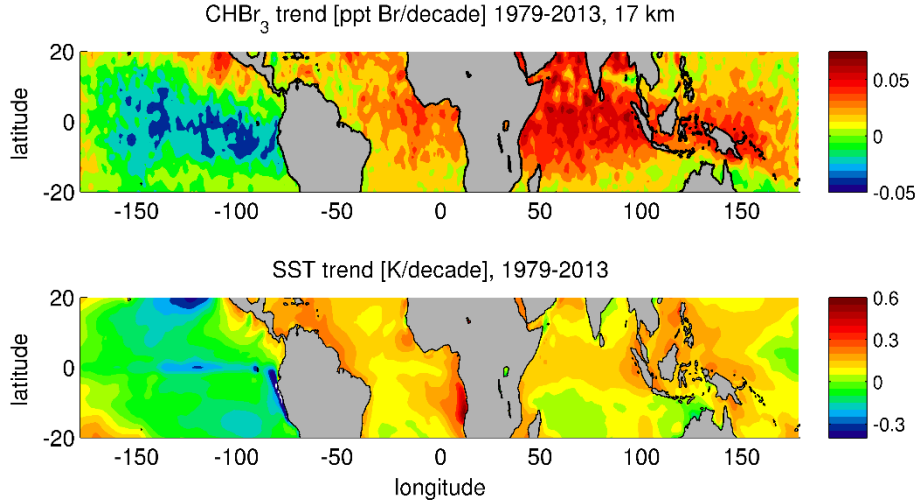


Figure 10. Modeled long-term change of FLEXPART CHBr₃ [ppt Br/decade] at 17 km and ERA-Interim sea surface temperature (SST) [K/decade] for the time period 1979-2013.

The overall pattern of long-term CHBr₃ changes at 17 km shows a strong similarity to the long-term changes in sea surface temperature derived from ERA-Interim data (Figure 10). While the global mean surface temperature has increased due to anthropogenic greenhouse gas emissions (Hegerl et al., 2007), the spatial pattern of global warming is more complex. Most regions exhibit a warming trend over the 35 year period, however, much of the eastern Pacific cooled. This cooling may either be related to an unusual strong manifestation of internal variability in the observations or may be caused by external, regional forcings (e.g., Wang et al., 2012; Luo et al., 2012). ERA-Interim long-term temperature changes over the tropical oceans show good agreement with HadCRUT, a combined dataset of instrumental temperature records, with only small differences (Simmons et al., 2014). Most interesting for our analysis is the correlation between the SST trends and the long-term changes of stratospheric CHBr₃ entrainment. Regions with large positive SST trends such as the Indian Ocean, East Atlantic and Maritime Continent coincide with regions where the CHBr₃ entrainment trend is strongest. The east Pacific, on the other hand, stands out as the region where the SST cooling trend coincides with decreasing CHBr₃ entrainment. While this relation holds for many oceanic regions, we also find outliers such as the southern Indian Ocean, where SST trends are around zero but CHBr₃ entrainment shows a strong positive trend. Based on our modelling approach, the interaction of two mechanisms causes the strong correlation between the SST and CHBr₃ trends. Higher sea surface temperatures and stronger surface winds force a larger flux of CHBr₃ out of the ocean

into the atmosphere (Ziska et al., 2013) and at the same time cause enhanced convection, transporting surface air masses into the TTL (Tegtmeier et al., 2015). As the cold point tropopause altitude shows no significant trend in radiosondes or ERA-Interim data over the 1980-2013 time period (Tegtmeier et al., 2020), CHBr₃ changes at 17 km correspond directly to changes of stratospheric CHBr₃ entrainment. Future SST changes can be expected to drive a continued positive trend of stratospheric CHBr₃ entrainment (Hossaini et al., 2012a).

3.6 Overall CH₂Br₂ and CHBr₃ contribution to stratospheric bromine

CHBr₃ together with CH₂Br₂ provides the main contribution of oceanic bromine to the stratosphere. CH₂Br₂ mixing ratios in the inner tropical belt (10°S-10°N) show less variability than CHBr₃, consistent with the longer lifetime, and range between 0.9 and 1.4 ppt. Largest values can be detected over the West and Central Pacific and are distributed evenly over both hemispheres (Figure 11). There is no local CH₂Br₂ maxima over the Indian Ocean, as observed for CHBr₃, since no strong localized sources in the region exist according to the Ziska et al., (2013) climatology. However, new ship measurements in the western Indian Ocean revealed high CH₂Br₂ surface water concentrations, i.e., south of Madagascar in July 2011 (Fiehn et al., 2017). Seasonal and interannual variations of CH₂Br₂ are much weaker than for CHBr₃ resulting in a continuous bromine entrainment into the stratosphere.

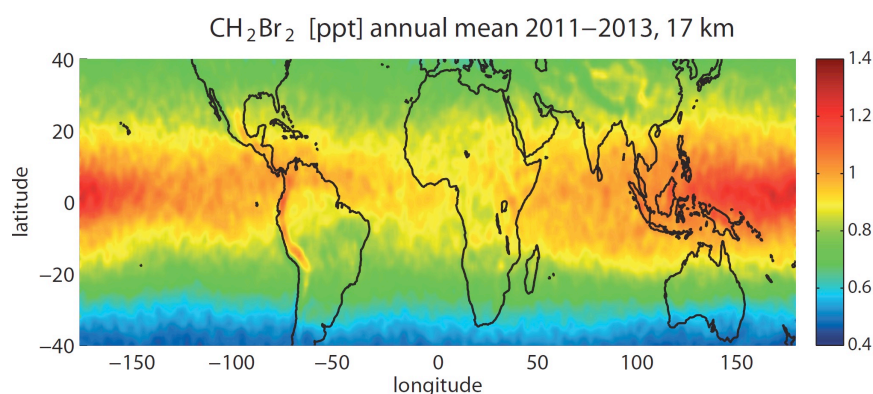


Figure 11. Modeled tropical annual mean distribution of CH₂Br₂ [ppt] at 17 km for 2011-2013.

Figure 12 shows the annual, tropical mean CHBr₃ and CH₂Br₂ profiles averaged over 1979-2013. At the surface, tropical mean values of 1 ppt CH₂Br₂ and 0.6 ppt CHBr₃ are simulated, which are slightly smaller than reported observations (Ziska et al., 2013 and references therein). Mixing ratios in the free troposphere decrease by nearly 50% (10%) for CHBr₃ (CH₂Br₂) when compared to the marine boundary layer. Both gases are well mixed in the free troposphere with nearly constant mixing ratios of 0.3 and 0.9 ppt for CHBr₃ and CH₂Br₂, respectively, corresponding to 0.9 ppt and 1.8 ppt bromine (Figure 12). CHBr₃ shows a slight S-shape with elevated abundances around 12-14 km related to strong convective outflow at this level bringing

marine boundary layer air directly into the lower TTL. Above 14 km, CHBr_3 mixing ratios start to decrease reaching values of 0.22 ppt at 17 km close to the cold point, corresponding to 0.66 ppt bromine. CH_2Br_2 mixing ratios, on the other hand, stay nearly constant up to 18 km, as expected based on its quite long lifetime of 400 to 500 days in the TTL, reaching values of 0.9 ppt (1.8 ppt bromine).

CHBr_3 profiles for four different regions (Figure 12) show that surface atmospheric mixing ratios are strongest in the Indian Ocean and Central America. Overall maximum mixing ratios over the Indian Ocean result from strong surface emissions combined with a relatively strong transport and main convective outflow between 11 and 14 km giving an S-shape CHBr_3 profile. Only for the West Pacific, transport into the stratosphere is more efficient, however, smaller emissions lead to the total entrainment over this region being smaller than over the Indian Ocean.

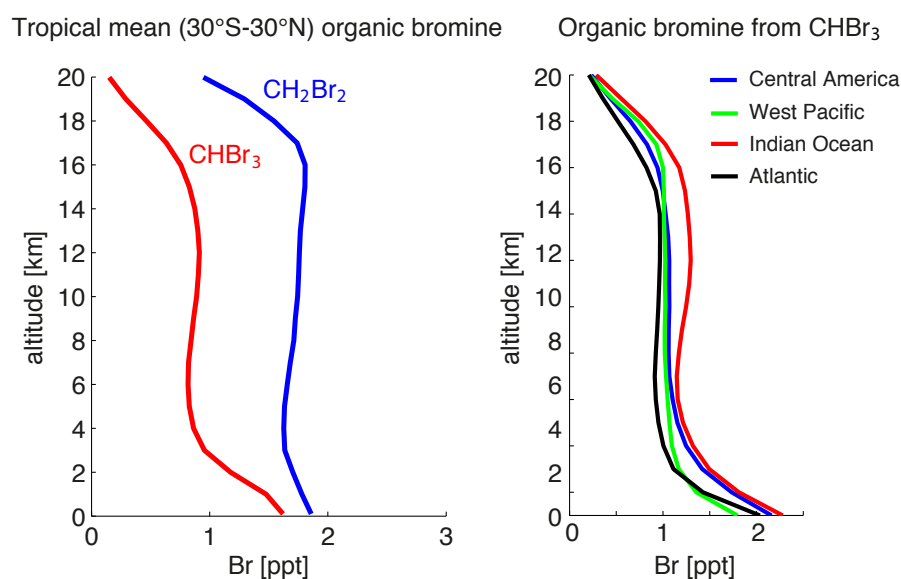


Figure 12. Modelled vertical profiles of CHBr_3 and CH_2Br_2 [ppt Br] in the tropics (30°S-30°N) (right panel) and of CHBr_3 for Central America (0°-20°N, 70°W-110°W), West Pacific (15°S-5°N, 140°E-150°W), Indian Ocean (0°-20°N, 40°E-110°E), and Atlantic (0°-20°N, 20°W-50°W) (right panel) for 1979-2013.

Table 2 gives the contribution of CHBr_3 and CH_2Br_2 to the stratospheric bromine loading based on source gas (SG) injection alone and based on the sum of source and product gas (PG)

injection. CHBr₃ and CH₂Br₂ have been evaluated directly at the cold point (as given by ERA-Interim) and contribute 2.4 ppt Br to stratospheric bromine loading directly in form of SG entrainment with 75% (25%) resulting from CH₂Br₂ (CHBr₃). The CHBr₃ estimates of 0.2 ppt (corresponding to 0.6 ppt Br) are in agreement with other studies which range from 0.1 ppt (Warwick et al., 2006; Aschmann et al., 2009) to 0.35 ppt (Hossaini et al., 2012b). For CH₂Br₂, our results of 0.9 ppt (corresponding to 1.8 ppt Br) agree very well with CTM modelling studies (Hossaini et al., 2012b) which give estimates of 0.75 – 0.9 ppt. The overall contribution of the two gases in form of SG and PG entrainment of 4.7 ppt is also in good agreement with earlier studies giving estimates ranging from 4-5 ppt (Hossaini et al., 2013) to 7.7 ppt (Liang et al., 2014).

Table 2. Modelled contribution of CHBr₃ and CH₂Br₂ to the stratospheric halogen loading in form of source gas (SG) and total (SG+PG) contribution for 2011-2013.

Br [ppt]	Inner tropics (10°S-10°N)		Tropics (30°S-30°N)	
	SG	SG+PG	SG	SG+PG
CHBr ₃	0.9	1.1	0.6	0.9
CH ₂ Br ₂	2.1	4.4	1.8	3.8
CHBr₃ + CH₂Br₂	3.0	5.5	2.4	4.7

A detailed comparison of our results over the eastern and western tropical Pacific to results derived from ATTREX and CONTRAST aircraft measurements and related model calculations is given in Table 3. Considering that CH₂Br₂ and CHBr₃ contribute >80% of the total SG Br in the TTL, our SG estimates agree very well with the measurements (Navarro et al., 2015; Werner et al., 2017; Wales et al., 2018). PG estimates are in general characterized by larger uncertainties. The PG contribution can be inferred from atmospheric measurements of BrO, the most abundant Br_y species, and the partitioning of inorganic Br_y derived from a photochemical model (König et al., 2017; Werner et al., 2017; Wales et al., 2018). Uncertainties in this method arise from modelling the Br_y partitioning and from uncertainties in measuring BrO and can be as large as ± 2.1 ppt (e.g., Wales et al., 2018).

Our study uses a simplified approach with a prescribed Br_y partitioning including its spatial and temporal variations. We have carried out sensitivity studies to analyse how variations of the Br_y partitioning impact the total amount of PG reaching the cold point tropopause (not shown here). Our studies show that uncertainties of 20% in the partitioning will lead to variations of ± 0.4 ppt in the PG entrainment. Such uncertainties in the Br_y partitioning can result from errors in the aerosols loading and in the heterogeneous reactions. Distributions of total Br_y and BrO in p-TOMCAT, the model used to derive the partitioning, have been shown to agree well with in-situ and satellite observations (Yang et al., 2005; 2010). If the uncertainties in the partitioning would be as large as 50%, the PG entrainment would show variations of ± 1.1 ppt. Overall the PG entrainment based on our simplified approach agrees very well (within $\pm 25\%$) with estimates from other studies derived from BrO measurements and photochemical modelling (Table 3).

~~measurements and model calculations reported in Navarro et al. (2015) and Wales et al. (2018). Navarro et al. (2015) reported measurements at the tropopause (17 km) of total VSL-Br of 5.24 ± 0.51 ppt in the Western tropical Pacific and 5.98 ± 1.95 ppt in the eastern tropical Pacific. Modelled PG for these conditions varied between 38 and 50% of the total VSL-Br. Also, Wales et al. (2018) estimated at total of 5.0 ± 2.1 ppt of total VSL-Br at the tropical Western Pacific Tropopause, which included 2.9 ± 0.6 ppt of SG Br and 2.1 ± 2.1 ppt of PG Br.~~

Table 3. Comparison of VSLs source gas (SG) contribution derived from this study and from aircraft measurements. Product gas (PG) contribution derived from this study and studies linking aircraft measurements and modelling.

Br [ppt]	Tropical eastern Pacific			Tropical western Pacific		
	SG	PG	SG+PG	SG	PG	SG+PG
This study	3	2.5	5.5	2.8	2.4	5.2
Navarro et al. (2015)	3 ± 0.4	3 ± 1.9	6 ± 1.9	3.3 ± 0.5	2 ± 0.2	5.2 ± 0.5
Werner et al. (2017)	3 ± 0.4	2.6 ± 1.0	5.6			
Wales et al. (2018)				2.9 ± 0.6	2.1 ± 2.1	5.0 ± 2.1

König et al. (2017)					2.6 ± 0.6	
---------------------	--	--	--	--	---------------	--

4 Discussion and summary

We combine observational data sets, including surface and upper air measurements, with high resolution atmospheric modelling in order to ~~analyse~~ **analyze** the spatial and temporal variability of VSLs entrainment into the stratosphere. Oceanic CHBr₃ in the TTL, on its way from the marine boundary layer into the stratosphere, shows a very high spatial and temporal variability. Regional maxima with mixing ratios of up to 0.4 to 0.5 ppt are simulated to be over Central America (1) and the Maritime Continent and tropical West Pacific (2), both of which are confirmed by high-altitude aircraft campaigns. The strongest stratospheric CHBr₃ entrainment is projected to occur over the region of India, Bay of Bengal and Arabian Sea (3), however, no data from aircraft campaigns are available to confirm this finding. Other tropical regions with only little convective uplift show smaller mixing ratios, mostly between 0.1 and 0.2 ppt. CHBr₃ fields on daily mean or shorter time scales is characterized by pronounced spatial variations with highly localized injections.

The modelled CHBr₃ maximum over Central America is caused by the co-occurrence of convectively driven short transport time scales and strong regional sources, with the latter being confirmed by data from various ship campaigns. Moreover, the combined seasonality of transport efficiency and emission strength causes the strong seasonality of CHBr₃ at 17 km over Central America. The model simulations also show a high spatial variability of CHBr₃ with strong latitudinal gradients, which is confirmed by available aircraft campaigns. The comparisons reveal that our model results are similar to the measurements for NH winter, but over- and underestimate (depending on the campaign) observations during NH summer, when the variability is largest. Exceptionally high CHBr₃ observed during the ACCENT campaign is also evident in the model results, but only in the daily and not in the monthly mean values. Given that individual campaigns may not be representative of mean values but may rather describe one side of the large spectrum, differences between model simulations and measurements, such as the ones discussed above, have to be interpreted with caution.

The modelled CHBr₃ maximum in the TTL over the West Pacific is centred south of the equator. This distribution cannot be explained by transport times scales, which are similar north and south of the equator and do not reveal strong hemispheric differences. Instead, strong oceanic sources south of equator, prescribed based on limited available measurements, are responsible for the high CHBr₃ mixing ratios in the SH. Measurements in the upper TTL from the ATTREX

aircraft campaign show an overall good agreement with model results, but also indicate that the model underestimates CHBr_3 in the tropics. Furthermore, ATTREX measurements did not show any significant gradient between the NH and SH tropics near the tropopause. Given the scarcity of in-situ measurements in the open ocean water of the West Pacific, it may be possible that oceanic emissions estimates used here are too low, especially north of the equator. Future ship campaigns are needed to confirm spatial and temporal differences and to improve existing bottom-up emission climatologies.

The overall strongest maximum over India, Bay of Bengal and Arabian Sea is caused by very large local sources. Transport from the ocean surface to 17 km is also efficient, but not strong enough to solely explain the pronounced maxima. No upper air measurements are available to back this upper TTL maximum and oceanic measurements used for the emission scenarios are also scarce. For the global tropical/extratropical distribution of CHBr_3 entrainment, largest uncertainties exist for estimated maxima in the region over India, Bay of Bengal and Arabian Sea. In situ measurements of the oceanic sources and the atmospheric distribution are needed to reduce local uncertainties and confirm global mean values.

Our understanding of stratospheric VSLS entrainment is also limited by the fact that currently available emission inventories do not take seasonal variations of oceanic concentrations into account.

Interannual variability of stratospheric CHBr_3 entrainment is to a large part driven by the variability of the coupled ocean-atmosphere circulation systems such as ENSO in the Pacific and IOD in the Indian Ocean. Long-term trends of the CHBr_3 entrainment, on the other hand, show a pronounced correlation with the SST trends. Both relations are based on the fact the stratospheric CHBr_3 entrainment is driven by strong sources and convective entrainment, which maximize for high surface temperatures and strong wind speeds. Following the SST trends, long term changes of CHBr_3 entrainment are positive in the West Pacific and Asian monsoon region but negative in the East Pacific. The tropical mean trend accounts for an increase of 0.017 ± 0.012 ppt Br/[decade](#) resulting in a 10% increase over the 1979-2013 time period. The overall contribution of CHBr_3 and CH_2Br_2 to the stratospheric halogen loading is 4.7 ppt Br with 50% being entrained in form of source gases, and the other 50% being entrained in form of product gases.

Data availability. The bromoform **and dibromomethane** emission inventory data (Ziska et al., 2013) are available at ACP/Pangaea and the FLEXPART model output can be inquired about by contacting the authors.

Author contributions. ST, KK, and BQ developed the idea for this paper and the model experiments. ST carried out the FLEXPART model calculations and the comparison to the aircraft observations. EA provided aircraft data. FZ compiled the Ziska et al. (2013) climatology for this study. ST wrote the manuscript with contributions from all co-authors.

Competing interests. The authors declare that they have no conflict of interest.

Acknowledgements This study was carried out within the BMBF project ROMIC THREAT (01LG1217A). ST was funded by ROMIC THREAT (01LG1217A) when compiling the study and by the Deutsche Forschungsgemeinschaft (DFG, German Research Foundation) – TE 1134/1 when writing the manuscript. EA was supported by grants from the NASA Upper Atmosphere. The authors are grateful to the ECMWF for making the reanalysis product ERA-Interim available.

References

- Aschmann, J., Sinnhuber, B.-M., Atlas, E. L. and Schauffler, S. M.: Modeling the transport of very short-lived substances into the tropical upper troposphere and lower stratosphere, *Atmospheric Chemistry and Physics*, 9(23), 2009.
- Aschmann, J., Sinnhuber, B.-M., Chipperfield, M. P., and Hossaini, R.: Impact of deep convection and dehydration on bromine loading in the upper troposphere and lower stratosphere, *Atmos. Chem. Phys.*, 11, 2671-2687, <https://doi.org/10.5194/acp-11-2671-2011>, 2011.
- Austin, J. N., and Butchart, N.: Coupled chemistry-climate model simulations for the period 1980 to 2020: ozone depletion and the start of ozone recovery, *Quarterly Journal of the Royal Meteorological Society*, 129: 3225–3249, 2006.
- Braesicke, P., Keeble, J., Yang, X., Stiller, G., Kellmann, S., Abraham, N. L., Archibald, A., Telford, P., and Pyle, J. A.: Circulation anomalies in the Southern Hemisphere and ozone changes, *Atmos. Chem. Phys.*, 13, 10677–10688, [doi:10.5194/acp-13-10677-2013](https://doi.org/10.5194/acp-13-10677-2013), 2013.
- Brinckmann, S., Engel, A., Bönisch, H., Quack, B., and Atlas, E.: Short-lived brominated hydrocarbons – observations in the source regions and the tropical tropopause layer, *Atmos. Chem. Phys.*, 12, 1213-1228, [doi:10.5194/acp-12-1213-2012](https://doi.org/10.5194/acp-12-1213-2012), 2012.
- Butler, J. H., King, D. B., Lobert, J. M., Montzka, S. A., Yvon-Lewis, S. A., Hall, B. D., Warwick, N. J., Mondeel, D. J., Aydin, M. and Elkins, J. W.: Oceanic distributions and emissions of short-lived halocarbons, *Global Biogeochemical Cycles*, 21(1), [doi:10.1029/2006GB002732](https://doi.org/10.1029/2006GB002732), 2007.
- Carpenter, L.J. and Reimann, S. (Lead Authors), J.B. Burkholder, C. Clerbaux, B.D. Hall, R. Hossaini, J.C. Laube, and S.A. Yvon-Lewis, Ozone-Depleting Substances (ODSs) and Other Gases of Interest to the Montreal Protocol, Chapter 1 in *Scientific Assessment of Ozone Depletion: 2014*, Global Ozone Research and Monitoring Project–Report No. 55, World Meteorological Organization, Geneva, Switzerland, 2014.
- Chipperfield, M. P.: New version of the TOMCAT/SLIMCAT off-line chemical transport model: Intercomparison of stratospheric tracer experiments, *Quarterly Journal of the Royal Meteorological Society*, 132(617), 1179–1203, [doi:10.1256/qj.05.51](https://doi.org/10.1256/qj.05.51), 2006.
- Dee, D. P., Uppala, S. M., Simmons, A. J., Berrisford, P., Poli, P., Kobayashi, S., Andrae, U., Balmaseda, M. A., Balsamo, G., Bauer, P., Bechtold, P., et al.: The ERA-Interim reanalysis: configuration and performance of the data assimilation system, *Quarterly Journal of the Royal Meteorological Society*, 137(656), 553–597, [doi:10.1002/qj.828](https://doi.org/10.1002/qj.828), 2011.
- Dorf, M., Butz, A., Camy-Peyret, C., Chipperfield, M. P., Kritten, L., and Pfeilsticker, K.: Bromine in the tropical troposphere and stratosphere as derived from balloon-borne BrO observations, *Atmos. Chem. Phys.*, 8, 7265-7271, [doi:10.5194/acp-8-7265-2008](https://doi.org/10.5194/acp-8-7265-2008), 2008.

Engel, A., Rigby, M. (Lead A., Burkholder, J. B., Fernandez, R. P., Froidevaux, L., Hall, B. D., Hossaini, R., Saito, T., Vollmer, M. K. and Yao, B.: Update on Ozone-Depleting Substances (ODSs) and Other Gases of Interest to the Montreal Protocol, Chapter 1, in Scientific Assessment of Ozone Depletion: 2018, Global Ozone Research and Monitoring Project – Report No. 58., 2018.

Fernandez, R. P., Salawitch, R. J., Kinnison, D. E., Lamarque, J.-F., and Saiz-Lopez, A.: Bromine partitioning in the tropical tropopause layer: implications for stratospheric injection, *Atmos. Chem. Phys.*, 14, 13391-13410, <https://doi.org/10.5194/acp-14-13391-2014>, 2014.

Fiehn, A., Quack, B., Hepach, H., Fuhlbrügge, S., Tegtmeier, S., Toohey, M., Atlas, E., and Krüger, K.: Delivery of halogenated very short-lived substances from the west Indian Ocean to the stratosphere during the Asian summer monsoon, *Atmos. Chem. Phys.*, 17, 6723-6741, <https://doi.org/10.5194/acp-17-6723-2017>, 2017.

Fiehn, A., Quack, B., Marandino, C. A., and Krüger, K., Transport variability of very short lived substances from the West Indian Ocean to the stratosphere. *Journal of Geophysical Research: Atmospheres*, 123, 5720– 5738. <https://doi.org/10.1029/2017JD027563>, 2018a.

Fiehn, A., Quack, B., Stemmler, I., Ziska, F., and Krüger, K.: Importance of seasonally resolved oceanic emissions for bromoform delivery from the tropical Indian Ocean and west Pacific to the stratosphere, *Atmos. Chem. Phys.*, 18, 11973–11990, <https://doi.org/10.5194/acp-18-11973-2018>, 2018b.

Forster, C., Stohl, A. and Seibert, P.: Parameterization of Convective Transport in a Lagrangian Particle Dispersion Model and Its Evaluation, *Journal of Applied Meteorology and Climatology*, 46(4), 403–422, doi:10.1175/JAM2470.1, 2007.

Forster, C., Wandinger, U., Wotawa, G., James, P., Mattis, I., Althausen, D., Simmonds, P., O'Doherty, S., Jennings, S. G., Kleefeld, C., Schneider, J., et al.: Transport of boreal forest fire emissions from Canada to Europe, *Journal of Geophysical Research*, 106(D19), 22887, doi:10.1029/2001JD900115, 2001.

Fuhlbrügge, S., Quack, B., Tegtmeier, S., Atlas, E., Hepach, H., Shi, Q., Raimund, S., and Krüger, K.: The contribution of oceanic halocarbons to marine and free tropospheric air over the tropical West Pacific, *Atmos. Chem. Phys.*, 16, 7569-7585, <https://doi.org/10.5194/acp-16-7569-2016>, 2016.

Hegerl, G.C., F. W. Zwiers, P. Braconnot, N.P. Gillett, Y. Luo, J.A. Marengo Orsini, N. Nicholls, J.E. Penner and P.A. Stott: Understanding and Attributing Climate Change. In: *Climate Change 2007: The Physical Science Basis. Contribution of Working Group I to the Fourth Assessment Report of the Intergovernmental Panel on Climate Change* [Solomon, S., D. Qin, M. Manning, Z. Chen, M. Marquis, K.B. Averyt, M. Tignor and H.L. Miller (eds.)]. Cambridge University Press, Cambridge, United Kingdom and New York, NY, USA, 2007

Hepach, H., Quack, B., Tegtmeier, S., Engel, A., Bracher, A., Fuhlbrügge, S., Galgani, L., Atlas, E. L., Lampel, J., Frieß, U., and Krüger, K.: Biogenic halocarbons from the Peruvian upwelling region as tropospheric halogen source, *Atmos. Chem. Phys.*, 16, 12219–12237, <https://doi.org/10.5194/acp-16-12219-2016>, 2016.

Hossaini, R., Chipperfield, M. P., Monge-Sanz, B. M., Richards, N. A. D., Atlas, E., and Blake, D. R.: Bromoform and dibromomethane in the tropics: a 3-D model study of chemistry and transport, *Atmos. Chem. Phys.*, 10, 719–735, <https://doi.org/10.5194/acp-10-719-2010>, 2010.

Hossaini, R., Chipperfield, M. P., Dhomse, S., Ordóñez, C., Saiz-Lopez, A., Abraham, N. L., Archibald, A. T., Braesicke, P., Telford, P., and Warwick, N.: Modelling future changes to the stratospheric source gas injection of biogenic bromocarbons, *Geophys. Res. Lett.*, 39, L20813, doi: 10.1029/2012GL053401, 2012a.

Hossaini, R., Chipperfield, M. P., Feng, W., Breider, T. J., Atlas, E., Montzka, S. A., Miller, B. R., Moore, F. and Elkins, J.: The contribution of natural and anthropogenic very short-lived species to stratospheric bromine, *Atmospheric Chemistry and Physics*, 12(1), 371–380, doi:10.5194/acp-12-371-2012, 2012b.

Hossaini, R., Mantle, H., Chipperfield, M. P., Montzka, S. A., Hamer, P., Ziska, F., Quack, B., Krüger, K., Tegtmeier, S., Atlas, E., Sala, S., Engel, A., Bönisch, H., Keber, T., Oram, D., Mills, G., Ordóñez, C., Saiz-Lopez, A., Warwick, N., Liang, Q., Feng, W., Moore, F., Miller, B. R., Marécal, V., Richards, N. A. D., Dorf, M., and Pfeilsticker, K.: Evaluating global emission inventories of biogenic bromocarbons, *Atmos. Chem. Phys.*, 13, 11819–11838, doi:10.5194/acp-13-11819-2013, 2013.

Hossaini, R., Chipperfield, M. P., Montzka, S. A., Rap, A., Dhomse, S., and Feng, W.: Efficiency of short-lived halogens at influencing climate through depletion of stratospheric ozone, *Nat. Geosci.*, 8, 186–190, doi:10.1038/ngeo2363, 2015.

Hossaini, R., Patra, P. K., Leeson, A. A., Krysztofiak, G., Abraham, N. L., Andrews, S. J., Archibald, A. T., Aschmann, J., Atlas, E. L., Belikov, D. A., Bönisch, H., Carpenter, L. J., Dhomse, S., Dorf, M., Engel, A., Feng, W., Fuhlbrügge, S., Griffiths, P. T., Harris, N. R. P., Hommel, R., Keber, T., Krüger, K., Lennartz, S. T., Maksyutov, S., Mantle, H., Mills, G. P., Miller, B., Montzka, S. A., Moore, F., Navarro, M. A., Oram, D. E., Pfeilsticker, K., Pyle, J. A., Quack, B., Robinson, A. D., Saikawa, E., Saiz-Lopez, A., Sala, S., Sinnhuber, B.-M., Taguchi, S., Tegtmeier, S., Lidster, R. T., Wilson, C., and Ziska, F.: A multi-model intercomparison of halogenated very short-lived substances (TransCom-VSLS): linking oceanic emissions and tropospheric transport for a reconciled estimate of the stratospheric source gas injection of bromine, *Atmos. Chem. Phys.*, 16, 9163–9187, doi:10.5194/acp-16-9163-2016, 2016.

Ko, M.K.W. and Poulet, G. (Lead Authors) Blake, D.R., Boucher, O., Burkholder, J.H., Chin, M., Cox, R.A., George, C., Graf, H.-F., Holton, J.R., Jacob, D.J., Law, K.S., Lawrence, M.G., Midgley, P.M., Seakins, P.W., Shallcross, D.E., Strahan, S.E., Wuebbles, D.J., and Yokouchi,

Y. (2002) Very short-lived halogen and sulfur substances. Chapter 2 in Scientific Assessment of Ozone Depletion: 2002 Global Ozone Research and Monitoring Project–Report No. 47, World Meteorological Organization, Geneva, Switzerland, 2003.

Krüger, K., Tegtmeier, S. and Rex, M.: Variability of residence time in the Tropical Tropopause Layer during Northern Hemisphere winter, *Atmos. Chem. Phys.*, 9(18), 6717–6725, 2009.

Liang, Q., Stolarski, R. S., Kawa, S. R., Nielsen, J. E., Douglass, A. R., Rodriguez, J. M., Blake, D. R., Atlas, E. L., and Ott, L. E.: Finding the missing stratospheric Br_y: a global modeling study of CHBr₃ and CH₂Br₂, *Atmos. Chem. Phys.*, 10, 2269–2286, doi:10.5194/acp-10-2269-2010, 2010.

Liang, Q., Atlas, E., Blake, D., Dorf, M., Pfeilsticker, K., and Schauffler, S.: Convective transport of very short lived bromocarbons to the stratosphere, *Atmos. Chem. Phys.*, 14, 5781–5792, <https://doi.org/10.5194/acp-14-5781-2014>, 2014.

Luo, J. J., W. Sasak ia, and Y. Masumoto: Indian Ocean warming modulates Pacific climate change, *Proc. Natl. Acad. Sci. U.S.A.*, 109, 18,701–18,706, doi:10.1073/pnas.1210239109, 2012.

Marandino, C. A., Tegtmeier, S., Krüger, K., Zindler, C., Atlas, E. L., Moore, F., and Bange, H. W.: Dimethylsulphide (DMS) emissions from the western Pacific Ocean: a potential marine source for stratospheric sulphur?, *Atmos. Chem. Phys.*, 13, 8427–8437, <https://doi.org/10.5194/acp-13-8427-2013>, 2013.

McLinden, C. A., Haley, C. S., Lloyd, N. D., Hendrick, F., Rozanov, A., Sinnhuber, B.-M., Goutail, F., Degenstein, D. A., Llewellyn, E. J., Sioris, C. E., Van Rozendael, M., Pommereau, J. P., Lotz, W., and Burrows, J. P.: Odin/OSIRIS observations of stratospheric BrO: Retrieval methodology, climatology, and inferred Br_y, *J. Geophys. Res.-Atmos.*, 115, D15308, doi:10.1029/2009JD012488, 2010.

Navarro, M. A., Atlas, E. L., Saiz-Lopez, A., Rodriguez-Lloveras, X., Kinnison, D. E., Lamarque, J.-F., Tilmes, S., Filus, M., Har- ris, N. R., and Meneguz, E.: Airborne measurements of organic bromine compounds in the Pacific tropical tropopause layer, *P. Natl. Acad. Sci. USA*, 112, 13789–13793, 2015.

Nightingale, P. D., Malin, G., Law, C. S., Watson, A. J., Liss, P. S., Liddicoat, M. I., Boutin, J. and Upstill-Goddard, R. C.: In situ evaluation of air-sea gas exchange parameterizations using novel conservative and volatile tracers, *Global Biogeochemical Cycles*, 14(1), 373–387, doi:10.1029/1999GB900091, 2000.

Ordóñez, C., Lamarque, J.-F., Tilmes, S., Kinnison, D. E., Atlas, E. L., Blake, D. R., Sousa Santos, G., Brasseur, G. and Saiz-Lopez, A.: Bromine and iodine chemistry in a global chemistry-climate model: description and evaluation of very short-lived oceanic sources, *Atmospheric Chemistry and Physics*, 12(3), 1423–1447, doi:10.5194/acp-12-1423-2012, 2012.

Pisso, I., Haynes, P. H., and Law, K. S.: Emission location dependent ozone depletion potentials for very short-lived halogenated species, *Atmos. Chem. Phys.*, 10, 12025–12036, doi:10.5194/acp-10-12025-2010, 2010.

Pyle, J. A., N. Warwick, X. Yang, P. J. Young, and G. Zeng: Climate/chemistry feedbacks and biogenic emissions, *Philos. Trans. R. Soc. A*, 365(1856), 1727–1740, doi:10.1098/rsta.2007.2041, 2007.

Quack, B., Wallace, D.W.R.: Air-sea flux of bromoform: Controls, rates, and implications. *Global Biogeochemical Cycles*, 17 (1), art. no.-GB1023, 2003.

Quack, B., E. Atlas, G. Petrick, and D. W. R. Wallace: Bromoform and dibromomethane above the Mauritanian upwelling: Atmospheric distributions and oceanic emissions, *J. Geophys. Res.*, 112(D9), D09312, doi:10.1029/2006JD007614, 2007.

Randel, W. J., Park, M., Emmons, L., Kinnison, D., Bernath, P., Walker, K. A., Boone, C., and Pumphrey, H.: Asian Monsoon Transport of Pollution to the Stratosphere, *Science*, 328, 611–613, doi:10.1126/science.1182274, 2010.

Saji, N. H., Goswami, B. N., Vinayachandran, P. N., and Yamagata, T.: A dipole made in the Tropical Indian Ocean. *Nature*. 401. 360-3. 10.1038/43854, 1999.

Salawitch, R. J.: Atmospheric chemistry: biogenic bromine, *Nature*, 439, 275–277, 2006.

Salawitch, Ross J. (Lead Author), David W. Fahey, Michaela I. Hegglin, Laura A. McBride, Walter R. Tribett, Sarah J. Doherty, Twenty Questions and Answers About the Ozone Layer: 2018 Update, Scientific Assessment of Ozone Depletion: 2018, 84 pp., World Meteorological Organization, Geneva, Switzerland, 2019.

Schmidt, J. A., et al., Modeling the observed tropospheric BrO background: Importance of multiphase chemistry and implications for ozone, OH, and mercury, *J. Geophys. Res. Atmos.*, 121, 11,819– 11,835, doi:10.1002/2015JD024229, 2016.

Simmons, A. J., Poli, P. , Dee, D. P., Berrisford, P. , Hersbach, H. , Kobayashi, S. and Peubey, C.: Estimating low-frequency variability and trends in atmospheric temperature using ERA-Interim. *Q.J.R. Meteorol. Soc.*, 140: 329-353. doi:10.1002/qj.2317, 2014.

Sinnhuber, B., and S. Meul: Simulating the impact of emissions of brominated very short lived substances on past stratospheric ozone trends. *Geophys. Res. Lett.*, 42, 2449–2456. doi: 10.1002/2014GL062975, 2015.

Sioris, C. E., et al.: Latitudinal and vertical distribution of bromine monoxide in the lower stratosphere from Scanning Imaging Absorption Spectrometer for Atmospheric Chartography limb scattering measurements, *J. Geophys. Res.*, 111, D14301, doi: 10.1029/2005JD006479, 2006.

Stemmler, I., Hense, I., and Quack, B.: Marine sources of bromoform in the global open ocean – global patterns and emissions, *Biogeosciences*, 12, 1967–1981, <https://doi.org/10.5194/bg-12-1967-2015>, 2015.

Stohl, A., Forster, C., Frank, A., Seibert, P. and Wotawa, G.: Technical note: The Lagrangian particle dispersion model FLEXPART version 6.2, *Atmospheric Chemistry and Physics*, 5(9), 2005.

Stohl, A., Hittenberger, M., and Wotawa, G.: Validation of the Lagrangian particle dispersion model FLEXPART against large-scale tracer experiment data, *Atmos. Environ.*, 32, 4245–4264, 1998.

Stohl, A. and Thomson, D. J.: A density correction for Lagrangian particle dispersion models, *BOUNDARY-LAYER METEOROLOGY*, 90(1), 155–167, doi:10.1023/A:1001741110696, 1999.

Stohl, A. and Trickl, T.: A textbook example of long-range transport: Simultaneous observation of ozone maxima of stratospheric and North American origin in the free troposphere over Europe, *Journal of Geophysical Research*, 104(D23), 30445, doi:10.1029/1999JD900803, 1999.

Stohl, A., Sodemann, H., Eckhardt, S., Frank, A., Seibert, P., and Wotawa, G.: The Lagrangian particle dispersion model FLEXPART version 8.2, Tech. rep., Norwegian Institute of Air Research (NILU), Kjeller, Norway, available at: <http://flexpart.eu/>, last access: 2 April 2020, 2010.

Tegtmeier, S., Krüger, K., Quack, B., Atlas, E. L., Pissio, I., Stohl, A. and Yang, X.: Emission and transport of bromocarbons: from the West Pacific ocean into the stratosphere, *Atmospheric Chemistry and Physics*, 12(22), 10633–10648, doi:10.5194/acp-12-10633-2012, 2012.

Tegtmeier, S., Krüger, K., Quack, B., Atlas, E., Blake, D. R., Boenisch, H., Engel, A., Hepach, H., Hossaini, R., Navarro, M. A., Raimund, S., Sala, S., Shi, Q., and Ziska, F.: The contribution of oceanic methyl iodide to stratospheric iodine, *Atmos. Chem. Phys.*, 13, 11869–11886, <https://doi.org/10.5194/acp-13-11869-2013>, 2013.

Tegtmeier, S., Ziska, F., Pissio, I., Quack, B., Velders, G. J. M., Yang, X., and Krüger, K.: Oceanic bromoform emissions weighted by their ozone depletion potential, *Atmos. Chem. Phys.*, 15, 13647–13663, doi:10.5194/acp-15-13647-2015, 2015.

Tegtmeier, S., Anstey, J., Davis, S., Dragani, R., Harada, Y., Ivanciu, I., Pilch Kedzierski, R., Krüger, K., Legras, B., Long, C., Wang, J. S., Wargan, K., and Wright, J. S.: Temperature and tropopause characteristics from reanalyses data in the tropical tropopause layer, *Atmos. Chem. Phys.*, 20, 753–770, <https://doi.org/10.5194/acp-20-753-2020>, 2020.

Tissier, A.-S. and Legras, B.: Convective sources of trajectories traversing the tropical tropopause layer, *Atmos. Chem. Phys.*, 16, 3383–3398, doi:10.5194/acp-16-3383-2016, 2016.

Wales, P. A., Salawitch, R. J., Nicely, J. M. Anderson, D. C., Canty, T. P., Baidar, S., et al., Stratospheric injection of brominated very short-lived substances: Aircraft observations in the Western Pacific and representation in global models. *Journal of Geophysical Research: Atmospheres*, 123. [https://doi.org/ 10.1029/2017JD027978](https://doi.org/10.1029/2017JD027978), 2018.

Wang, B., J. Liu, H. J. Kim, P. J. Webster, and S. Y. Yim: Recent change of the global monsoon precipitation (1979–2008), *Clim. Dyn.*, 39, 1123–1135, doi:10.1007/s00382-011-1266-z, 2012.

Warwick, N. J., J. A. Pyle, G. D. Carver, X. Yang, N. H. Savage, F. M. O'Connor, and R. A. Cox: Global modeling of biogenic bromocarbons, *J. Geophys. Res.*, 111, D24305, doi:10.1029/2006JD007264, 2006.

Werner, B., Stutz, J., Spolaor, M., Scalone, L., Raecke, R., Festa, J., Colosimo, S. F., Cheung, R., Tsai, C., Hossaini, R., Chipperfield, M. P., Taverna, G. S., Feng, W., Elkins, J. W., Fahey, D. W., Gao, R.-S., Hints, E. J., Thornberry, T. D., Moore, F. L., Navarro, M. A., Atlas, E., Daube, B. C., Pittman, J., Wofsy, S., and Pfeilsticker, K.: Probing the subtropical lowermost stratosphere and the tropical upper troposphere and tropopause layer for inorganic bromine, *Atmos. Chem. Phys.*, 17, 1161–1186, <https://doi.org/10.5194/acp-17-1161-2017>, 2017.

Wolter, K. and Timlin, M. S.: El Niño/Southern Oscillation behaviour since 1871 as diagnosed in an extended multivariate ENSO index (MEI.ext). *Int. J. Climatol.*, 31: 1074–1087. doi:10.1002/joc.2336, 2011.

Yamamoto, H., Yokouchi, Y., Otsuki, A., and Itoh, H.: Depth profiles of volatile halogenated hydrocarbons in seawater in the Bay of Bengal, *Chemosphere*, 45, 371–377, doi:10.1016/s0045- 6535(00)00541-5, 2001.

Yang, X., Cox, R. A., Warwick, N. J., Pyle, J. A., Carver, G. D., O'Connor, F. M., and Savage, N. H.: Tropospheric bromine chemistry and its impacts on ozone: A model study, *J. Geophys. Res.*, 110, D23311, doi:10.1029/2005JD006244, 2005.

Yang, X., Pyle, J. A., Cox, R. A., Theys, N., and Van Roozendael, M.: Snow-sourced bromine and its implications for polar tropospheric ozone, *Atmos. Chem. Phys.*, 10, 7763–7773, doi:10.5194/acp-10-7763-2010, 2010.

Yang, X., Abraham, N. L., Archibald, A. T., Braesicke, P., Keeble, J., Telford, P. J., Warwick, N. J., and Pyle, J. A.: How sensitive is the recovery of stratospheric ozone to changes in concentrations of very short-lived bromocarbons?, *Atmos. Chem. Phys.*, 14, 10431–10438, doi:10.5194/acp-14-10431-2014, 2014.

Ziska, F., Quack, B., Abrahamsson, K., Archer, S. D., Atlas, E., Bell, T., Butler, J. H., Carpenter, L. J., Jones, C. E., Harris, N. R. P., Hepach, H., et al.: Global sea-to-air flux climatology for bromoform, dibromomethane and methyl iodide, *Atmospheric Chemistry and Physics Discussions*, 13(2), 5601–5648, doi:10.5194/acpd-13-5601-2013, 2013.

Ziska, F., Quack, B., Tegtmeier, S., Stemmler, I., and Krüger, K.: Future emissions of marine halogenated very-short lived substances under climate change. *Journal of Atmospheric Chemistry*, 74: 245. <https://doi.org/10.1007/s10874-016-9355-3>, 2017.